

Geological Field Trips and Maps

2020

Vol. 12 (2.3)



ISSN: 2038-4947



**The submarine dune field of the Bolognano Fm:
depositional processes and the carbonate reservoir potential
(Chattian to Burdigalian, Majella Carbonate Platform)**

**Tidalites 2021 - 10th Congress of Tidal Sedimentology. Matera, Italy, 5-7 October 2021.
Field Trip T6 – Central Apennine – Maiella.**

<https://doi.org/10.3301/GFT.2020.05>

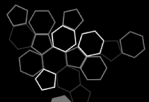


*Società Geologica
Italiana*



ISPRA

Dipartimento per il
SERVIZIO GEOLOGICO D'ITALIA
Organo Cartografico dello Stato (legge n°68 del 2-2-1960)



**Sistema Nazionale
per la Protezione
dell'Ambiente**

GFT&M - Geological Field Trips and Maps

Periodico semestrale del Servizio Geologico d'Italia - ISPRA e della Società Geologica Italiana
 Geol. F. Trips Maps, Vol. **12** No.2.3 (2020), 42 pp., 22 Figs. (<https://doi.org/10.3301/GFT.2020.05>)

The submarine dune field of the Bolognana Fm: depositional processes and the carbonate reservoir potential (Chattian to Burdigalian, Majella Carbonate Platform)

Tidalites 2021 - 10th Congress of Tidal Sedimentology. Matera, Italy, 5-7 October 2021.
Field Trip T6 – Central Apennine – Maiella.

Marco Brandano^{1,2}, Laura Tomassetti¹, Irene Cornacchia³, Fabio Trippetta¹, Luis Pomar⁴, Lorenzo Petracchini²

¹ Dipartimento di Scienze della Terra – Sapienza Università di Roma, P. le Aldo Moro 5 00185 Roma, Italy

² Istituto di Geologia Ambientale e Geoingegneria, IGAG-CNR, P. le Aldo Moro 5 00185, Roma, Italy

³ Istituto di Geoscienze e Georisorse IGG-CNR, Via G. Moruzzi 1 56124, Pisa, Italy

⁴ C àtedra Guillem Colom, University of the Balearic Islands, Ctra. Valldemossa, Km 7.5, E-07122 Palma de Mallorca, Spain

Corresponding Author e-mail address: marco.brandano@uniroma1.it

Responsible Director

Claudio Campobasso (ISPRA-Roma)

Editor in Chief

Andrea Zanchi (Università di Milano-Bicocca)

Editorial Manager

Valentina Campo (ISPRA-Roma) - *corresponding manager*,
Silvana Falchetti (ISPRA-Roma),
Fabio Massimo Petti (Società Geologica Italiana - Roma),
Alessandro Zuccari (Società Geologica Italiana - Roma)

Associate Editors

M. Berti (Università di Bologna), *M. Della Seta* (Sapienza Università di Roma),
P. Gianolla (Università di Ferrara), *G. Giordano* (Università Roma Tre),
M. Massironi (Università di Padova), *M.L. Pampaloni* (ISPRA-Roma),
M. Pantaloni (ISPRA-Roma), *M. Scambelluri* (Università di Genova),
S. Tavani (Università di Napoli Federico II)

Technical Advisory Board for Geological Maps

F. Capotorti (ISPRA-Roma), *F. Papasodaro* (ISPRA-Roma),
D. Tacchia (ISPRA-Roma), *S. Grossi* (ISPRA-Roma),
M. Zucali (University of Milano), *S. Zanchetta* (University of Milano-Bicocca),
M. Tropeano (University of Bari), *R. Bonomo* (ISPRA-Roma)

Editorial Advisory Board

D. Bernoulli, *F. Calamita*, *W. Cavazza*, *F.L. Chiocci*, *R. Compagnoni*,
D. Cosentino, *S. Critelli*, *G.V. Dal Piaz*, *P. Di Stefano*, *C. Doglioni*,
E. Erba, *R. Fantoni*, *M. Marino*, *M. Mellini*, *S. Milli*,
E. Chiarini, *V. Pascucci*, *L. Passeri*, *A. Peccerillo*, *L. Pomar*,
P. Ronchi, *B.C. Schreiber*, *L. Simone*, *I. Spalla*, *L.H. Tanner*,
C. Venturini, *G. Zuffa*.

Cover page Figure: Compound cross stratified character of the Lepidocyclina calcarenites 2 (Burdigalian, Bolognana Fm).

ISSN: 2038-4947 [online]

<http://gftm.socgeol.it/>

The Geological Survey of Italy, the Società Geologica Italiana and the Editorial group are not responsible for the ideas, opinions and contents of the guides published; the Authors of each paper are responsible for the ideas, opinions and contents published.

Il Servizio Geologico d'Italia, la Società Geologica Italiana e il Gruppo editoriale non sono responsabili delle opinioni espresse e delle affermazioni pubblicate nella guida; l'Autore/i è/sono il/i solo/i responsabile/i.

INDEX

Information

Abstract	4
Program summary	4
List of Stops	5
Safety	5

Excursion notes

Geological Setting	8
Early Miocene paleoceanographic setting	14
Oil shows and Bitumens in the Majella Area	15

Itinerary

DAY 1	18
Stop T6.1.1 - Panoramic view of Majella Carbonate Platform from Blockhaus and Monte Cavallo (42°08'42.21"N, 14°06'39.76"E)	18
Stop T6.1.2 - Valle dell'Orfento, the Decontra stratigraphic sections (42°09'46.78"N; 14°02'21.80"E)	20
Stop T6.1.3 - Panoramic view of S. Bartolomeo Valley (42°10'52.70"N; 14°02'05.61"E).....	23
DAY 2	25
Stop T6.2.1 - Piano delle Cappelle – Dune field (42°13'00.21"N; 14°04'18.17"E).....	25
Stop T.6.2.2 - Acquafredda Mines (42°12'14.08"N; 14°03'49.24"E).....	29
Stop T6.2.3 - Valle Romana Quarry (42°14'23.73"N; 14°03'26.00"E).....	31
Concluding remarks on dune field development	35
References	37

Abstract

This two-days field trip is focused on the Bolognano Formation, the homoclinal carbonate ramp developed on the Majella Mountain (Central Apennines) from the late Rupelian to the Messinian. The northern sectors of the Majella Mountain show excellent and continuous exposures of this carbonate ramp. In the late Oligocene-early Miocene, the paleoceanography of the Mediterranean was controlled by different seaways, one of the largest being the proto-Adriatic basin, bounded by the Apulian carbonate platform and by the Dinaride coast. In this context, a strong northward current led to the development of submarine dunes during the Chattian and the Burdigalian. In this fieldtrip, we discuss the relationships among sedimentary structures and depositional processes, stratigraphic architecture and syn/post-depositional tectonics. Furthermore, the lower Miocene cross-bedded calcarenites of the Bolognano Fm identify an important reservoir rock. In the last two stops, the bitumen shows are analysed and the possible controlling factors of migration and trapping are discussed. The comparison between bitumen-filled fractured and unfractured rocks allows detecting the controlling factors on the migration of the hydrocarbons and its relationship with tectonics. The high primary porosity and the lateral continuity of the calcarenites are identified as the main controlling factor on the hydrocarbon migration.

Keywords

Carbonate ramp, seaway, oceanography, hydrocarbons, carbonate reservoir.

Program summary

The northern sectors of Majella Mountain are incised by long valleys (e.g. Orfento and S. Spirito valleys), which allow to investigate the spectacular continuous exposures of Oligo-Miocene carbonate ramp deposits (Bolognano Fm), with particular attention to the facies changes both along and across the ramp environment. The Bolognano Fm offers the possibility to explore the sedimentary record of changing environmental conditions of the Mediterranean, which controlled the development of a homoclinal carbonate ramp between the late Rupelian and the early Messinian. In particular, the oceanographic conditions of the Mediterranean during the Rupelian-Chattian and the Burdigalian intervals promoted the development of a wide submarine dune field in the middle and outer ramp environment (Brandano et al., 2012; 2016a; 2017). In this field trip the

relationships among sedimentary structures and depositional processes, among stratigraphic architecture and syn/post-depositional tectonics are investigated and discussed.

Pores of the Bolognano Fm in the northern sector of Majella are locally filled with bitumen at different stratigraphic levels. However, most of the bitumen-bearing portions pertains to a specific member of the Bolognano Fm (*Lepidocyclina* Calcarenite 2) that is characterized by cross bedded calcarenites, which developed in the Aquitanian/Burdigalian submarine dune field (Lipparini et al., 2018; Trippetta et al., 2020). In the last two stops of the field trip, the bitumen shows are analysed and the possible controlling factors of migration and trapping are discussed.

List of Stops (Fig. 1)

1st Day

Stop T6.1.1 - Panoramic view of Majella Carbonate Platform from Blockhaus and Monte Cavallo;

Stop T6.1.2 - Valle dell'Orfento – Decontra stratigraphic sections;

Stop T6.1.3 - Panoramic view of S. Bartolomeo Valley

2nd Day

Stop T6.2.1 - Piano delle Cappelle – Dune field;

Stop T6.2.2 - Acqua Fredda mines;

Stop T6.2.3 - Valle Romana quarry.

Safety

Safety in the field is closely related to awareness of potential difficulties, fitness and use of appropriate equipment. Safety is a personal responsibility and all participants should be aware of the following issues. The excursion takes place at relatively low altitude (around 1000 m). Most of the outcrops are along road, trail and caves. Roads are in good condition, although to reach the outcrops it will be necessary to drive along very sinuous roads. We recommend to all participants to wear comfortable walking boots or at least lightweight hiking shoes. Trainers or running shoes are unsuitable footwear in the field. Since rain is possible in October, a waterproof coat/jacket is essential, while waterproof over-trousers may be useful. A small rucksack is needed for daily use to carry your waterproofs, a spare T-Shirt (and may be a fleece/sweater), a bottle of water and small snacks.

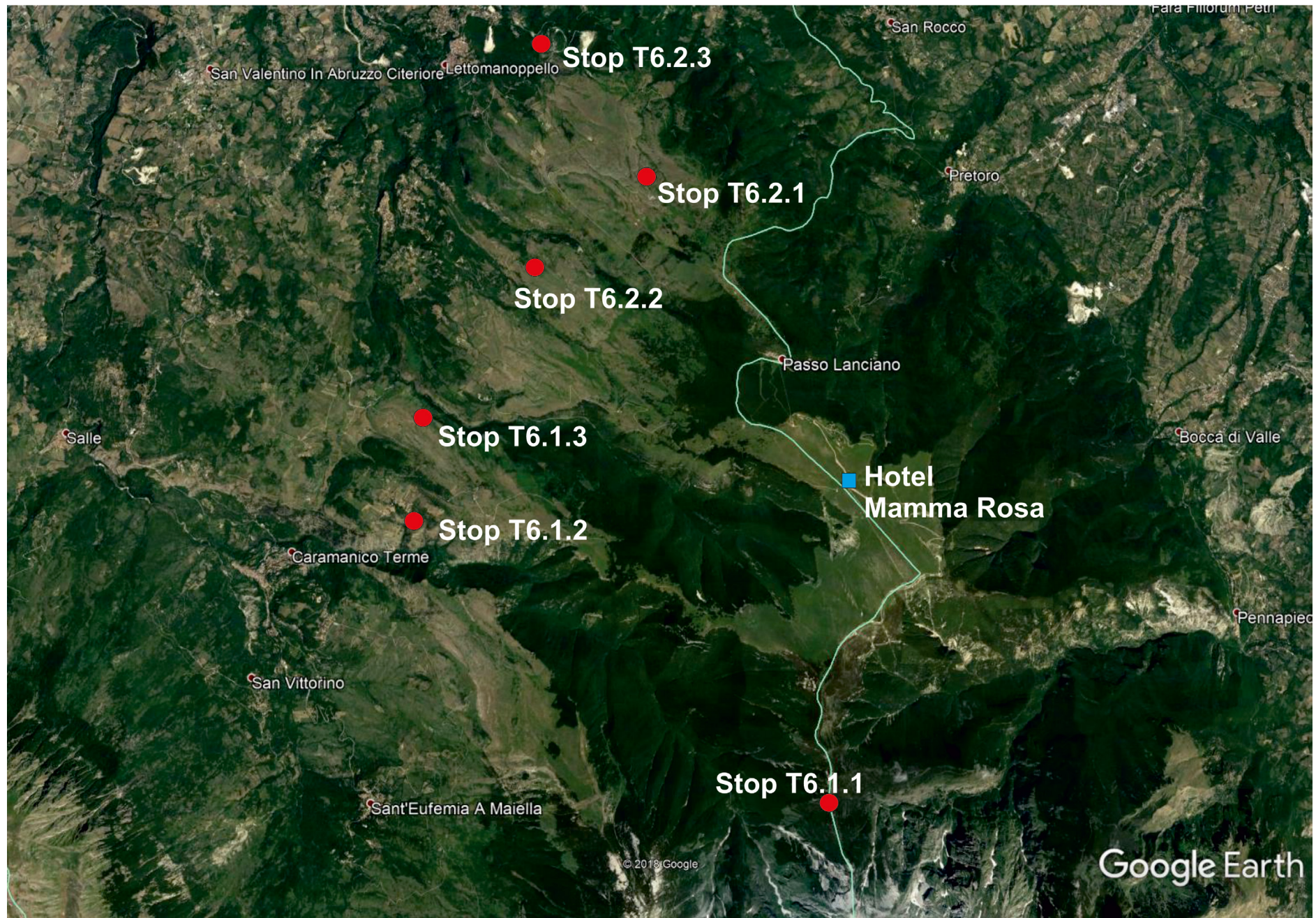


Fig. 1: Google Earth view of the itinerary of the field trip with locations of the stops.

Sun protection can be useful; hats or headscarves are useful. Participants should inform the excursion leaders (in confidence) of any physical or mental condition, which may affect performance in the field (e.g. asthma, diabetes, epilepsy, vertigo, heart condition, back problems, carsickness, lung disease, allergies etc.). Special diets are available on request (vegetarian, etc.). Mobile/cellular phone coverage is generally good, although in some place it can be absent.

Hospitals and first-aid stations

Ospedale Santissima Annunziata, Via dei Vestini 31, 66100 Chieti (CH); tel: +39 0871358539.

First aid station of Manoppello, Corso Santarelli 70, 65024 Manoppello (PE); tel: +39 085859700.

Accommodation

Albergo Mamma Rosa, Via SS Majelletta 35, 66010 Pretoro (CH); tel: +39 0871896144.



Geological Setting

The Majella Mountain belongs to the central Apennine fold and thrust belt. It consists of a 35 km long, N-S/NW-SE oriented thrust related anticline plunging both northward and southward (Fig. 2) (Vezzani and Ghisetti, 1998). The Majella sedimentary succession is characterised by Upper Jurassic to upper Miocene limestones and dolostones belonging to the Apulia Carbonate Platform (Crescenti et al., 1969), a large isolated platform established on the southern passive margin of the Mediterranean Tethys (Eberli et al., 1993; Bosellini, 2002). During the Mesozoic, a steep, non-depositional escarpment divided the platform from the northward extended basin (Fig. 3; Vecsei et al., 1998). Since the late Campanian, a large carbonate wedge prograded onto the basin that was infilled by onlapping sediments allowing the progradation of the platform that evolved into a distally steepened ramp (Orfento Fm) (Mutti et al., 1997; Vecsei et al., 1998). Recently, Eberli et al. (2019) on the basis of facies characters and association, interpreted the bioclastic wedge of the Orfento Fm as a carbonate delta drift. The top of the Orfento Fm is marked by an erosional unconformity overlain by pelagites alternating with breccias with lithoclasts and biodeprital grainstones of the Santo Spirito Fm (Vecsei et al., 1998). During the early Priabonian, small and scattered patch reefs developed in the northern Majella (Vecsei et al., 1998), while since Rupelian corals built mounded cluster reefs (Pescofalcone Fm) in the mesophotic zone, prograding up to 4 km basinward over the gently inclined upper slope (Brandano et al., 2019). From the late Rupelian to early Messinian interval, a persisting carbonate ramp, known as Bolognano Fm, developed above the carbonate ramp of the Santo Spirito Fm through a discontinuity surface (Mutti et al., 1997; Brandano et al., 2012; 2016a). The Bolognano Fm carbonate ramp ended with the sedimentation of the *Turborotalita multiloba* marls (Carnevale et al., 2011) and the Gessoso-Solfifera Fm (Crescenti et al., 1969). Finally, in the early Pliocene, the Majella carbonate ramp was involved into the tectonic development of the Apennine foredeep system linked to the Apennine orogeny (Cosentino et al., 2010).

Tectonic setting

The Majella Mountain is a broad east-verging thrust-related anticline located in the central Apennines at 35 km from the Adriatic coast in the Abruzzo region (Fig. 2). The Majella anticline is characterized by an arcuate shape (plunging both to the north and to the south) with the fold axis oriented NW-SE in its northern sector and N-S in the southern part. The Majella anticline extends northward in the subsurface for a distance > 40 km (Ghisetti and Vezzani, 2002).

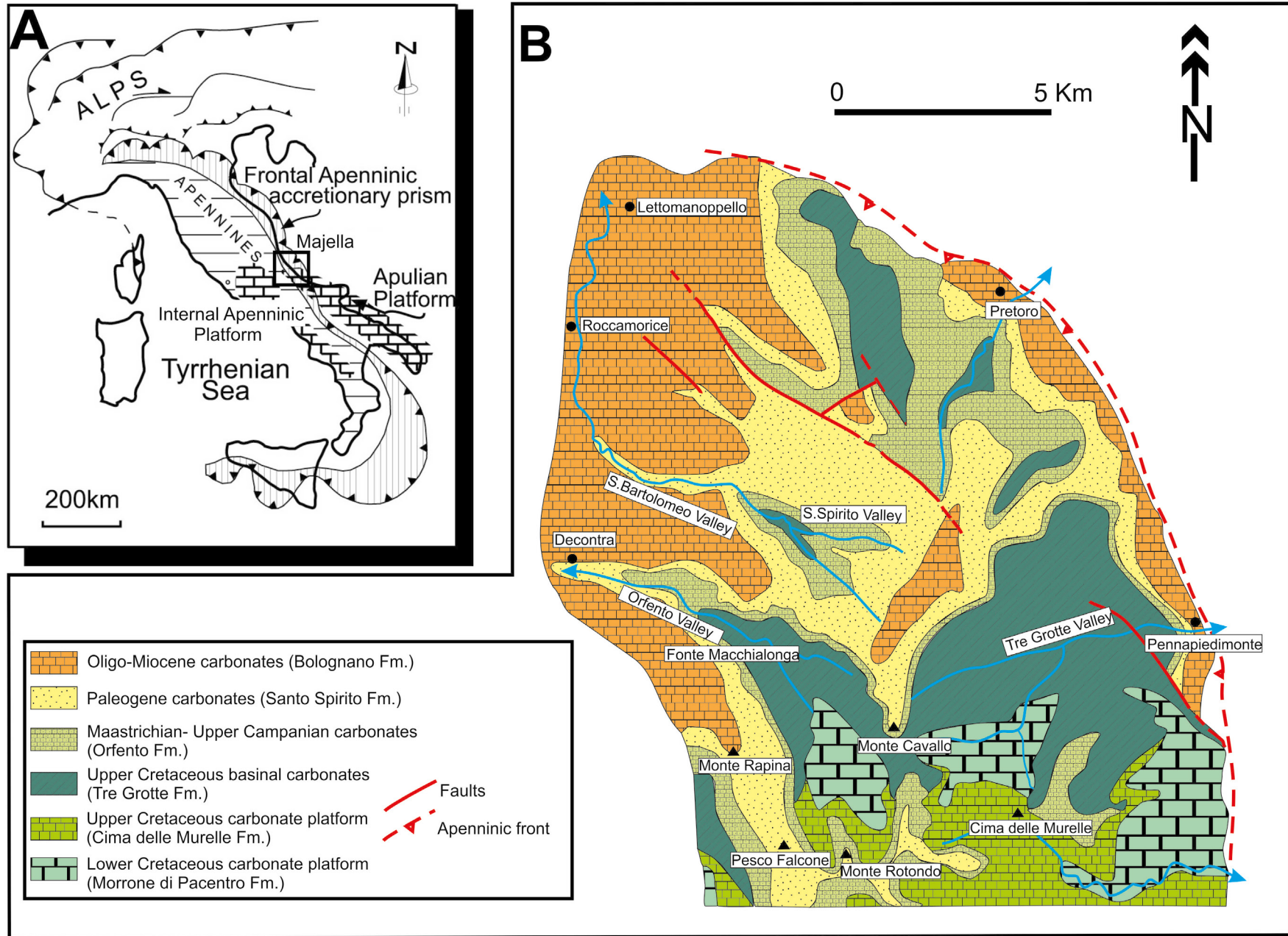


Fig. 2: A) Schematic geological map of Italy (modified after Doglioni and Brandano et al., 2016a, 1994). B) Simplified geological map of the Majella Mountain (modified after Vecsei and Sanders, 1999).

The Majella Mountain is delimited to the east by a regional west-dipping thrust, curved in shape, showing several kilometres of displacement with the Upper Jurassic to Miocene carbonates overlapping younger units (Ghisetti and Vezzani, 2002; Rustichelli et al., 2012). The eastern flank is steeply dipping and overturned in the central part, whereas a more symmetric geometry characterizes the northern and the southern anticline forelimb (Ghisetti and Vezzani, 2002).

The Majella backlimb is crosscut to the west by the Caramanico Fault, a west-dipping major normal fault with a maximum estimated normal throw up to 3.8-4.2 km (e.g., Ghisetti and Vezzani, 2002; Scisciani et al., 2002; Patacca et al., 2008).

The internal structure of the Majella Mountain is dissected by several faults characterized predominantly by normal and strike-slip kinematics with oblique slip components and subordinately reverse kinematics (Graham et al., 2003; Marchegiani et al., 2006; Antonellini et al., 2008; Rustichelli et al., 2012; Brandano et al., 2013). Most of the faults affecting the Upper Jurassic to Miocene carbonates in the Majella anticline are characterized by a displacement ranging from a few centimetres to several hundreds of meters (Rustichelli et al., 2012;

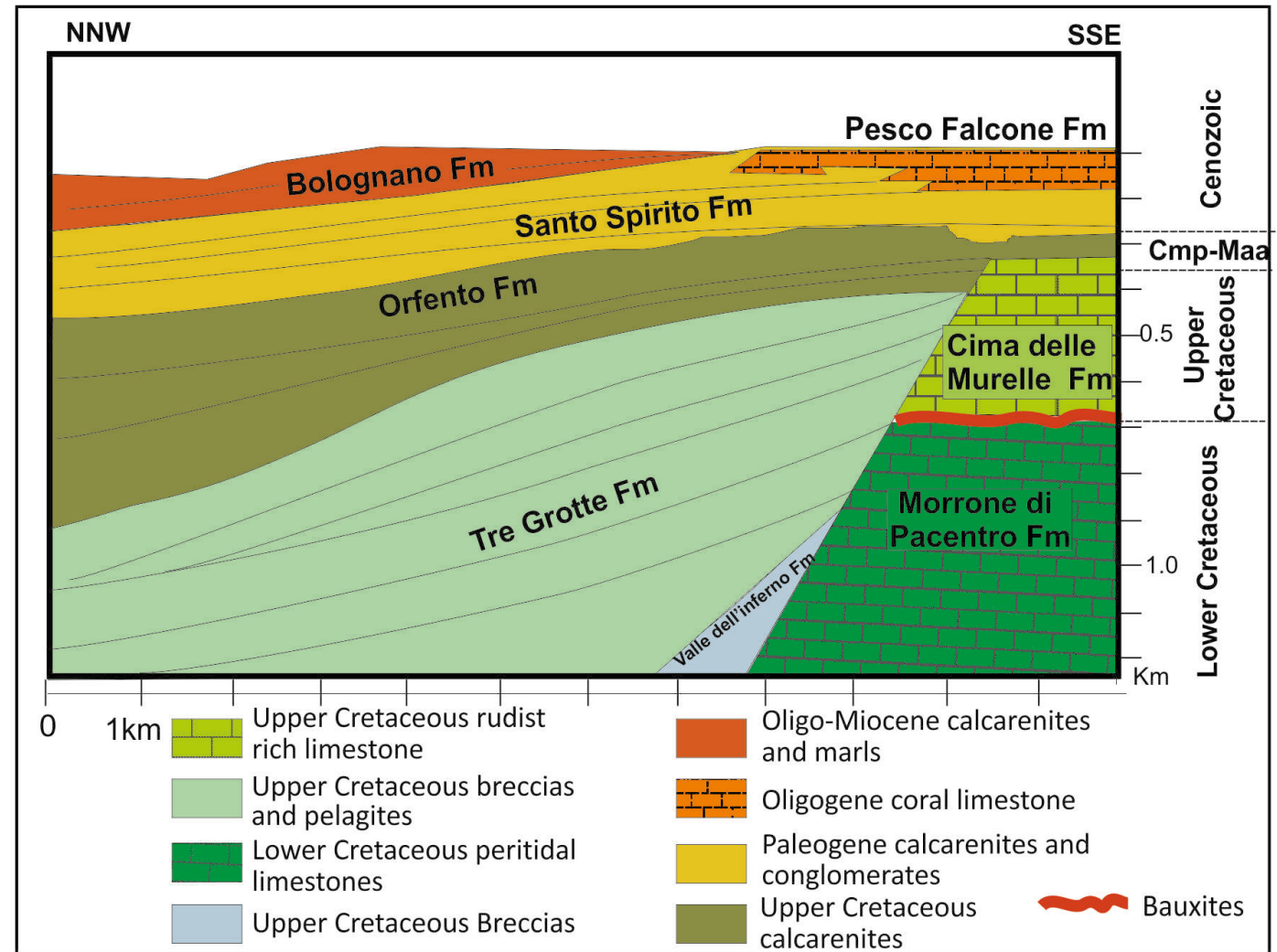


Fig. 3: Schematic architecture of the Majella Mountain carbonate platform (modified and redrawn after Vecsei et al., 1998).



Marchegiani et al., 2006; Tondi et al., 2006). The northern sector of the Majella Mountain (i.e. the area of the present work) is mostly crosscut by normal and strike-slip faults with a NW-SE trend (Fig. 2; Marchegiani et al., 2006; Agosta et al., 2009; Brandano et al., 2013).

Different interpretations have been proposed for the tectonic evolution of the Majella Mountain (Ghisetti and Vezzani, 2002; Scisciani et al., 2002), however in the literature the development of the anticline is generally set in the middle Pliocene till the late Pliocene (Ghisetti and Vezzani, 2002; Scisciani et al., 2002; Marchegiani et al., 2006; Patacca et al., 2008).

Stratigraphic architecture of Bolognano Fm

The Bolognano Fm represents an homoclinal carbonate ramp that developed above the S. Spirito Fm deposits (Mutti et al., 1997; Brandano et al., 2012; 2016a). The Bolognano Fm is constituted by six lithostratigraphic units, three of them are representative of shallow-water carbonates, alternating with deeper carbonate units (Brandano et al., 2016a) (Fig. 4). The first shallow water stage is represented by the *Lepidocyclina* Calcarenite 1 unit, deposited at the end of the Rupelian and lasted until the Chattian. It is mainly represented by cross-bedded bioclastic packstones dominated by larger benthic foraminifera (Fig. 5A) forming a large down-slope migrating dune field, developed within the middle ramp environment. The second unit is represented by Cherty Marly Limestones (Chattian-upper Aquitanian), in which the dominant skeletal components are planktonic foraminifera and sponge spicules (Fig. 5B). This unit records a drowning event that produced a sharp facies shift towards the low-energy outer ramp environment. At the base of the Burdigalian, the recovery of the carbonate ramp occurs, as testified by the deposition of the *Lepidocyclina* Calcarenite 2 (Fig. 5C, D), that once again indicates the development of a well-developed dune field within the middle ramp environment. The occurrence of a hardground surface marks the end of *Lepidocyclina* Calcarenite 2 deposition. In late Burdigalian, a second drowning event is recorded and marked by the deposition of two different lithostratigraphic units: the Bryozoan Calcarenites (Fig. 5E), in the Orfento Valley, and the Hemipelagic Calcareous Marls and Marly Limestone in the northern sector of the Majella Mountain, both representing the upper Burdigalian-Serravallian interval. The hemipelagic marly limestones unit consists of bioturbated packstones to packstones/wackestones rich in planktonic foraminifera and, subordinately, in small benthic foraminifera, echinoids and mollusc fragments (Fig. 5F). The last shallow-water stage is represented by the *Lithothamnion* Limestone unit (Tortonian), which is dominated by red algae assemblages (Fig. 5G, H). The *Lithothamnion* Limestone is interpreted to represent

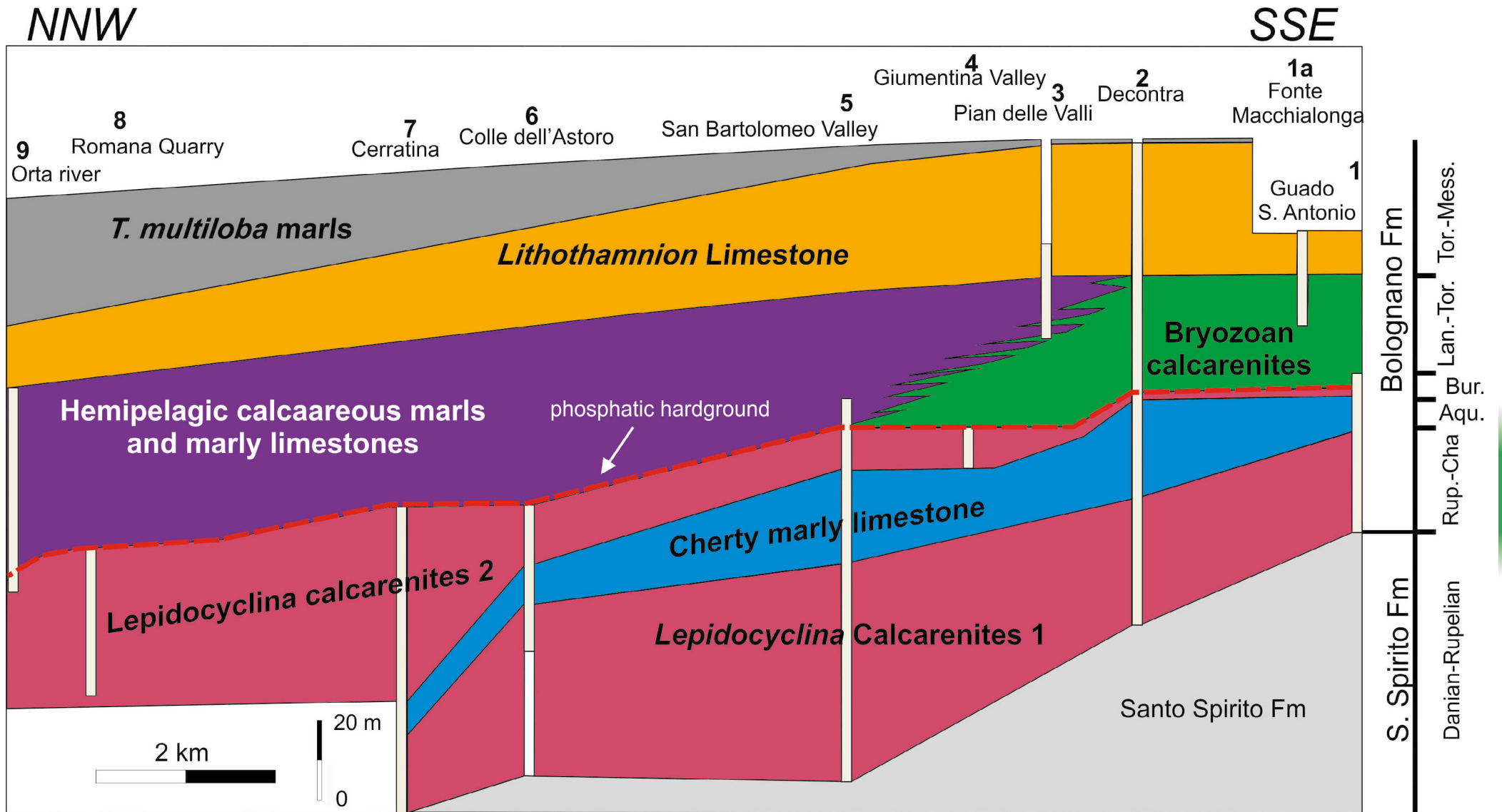
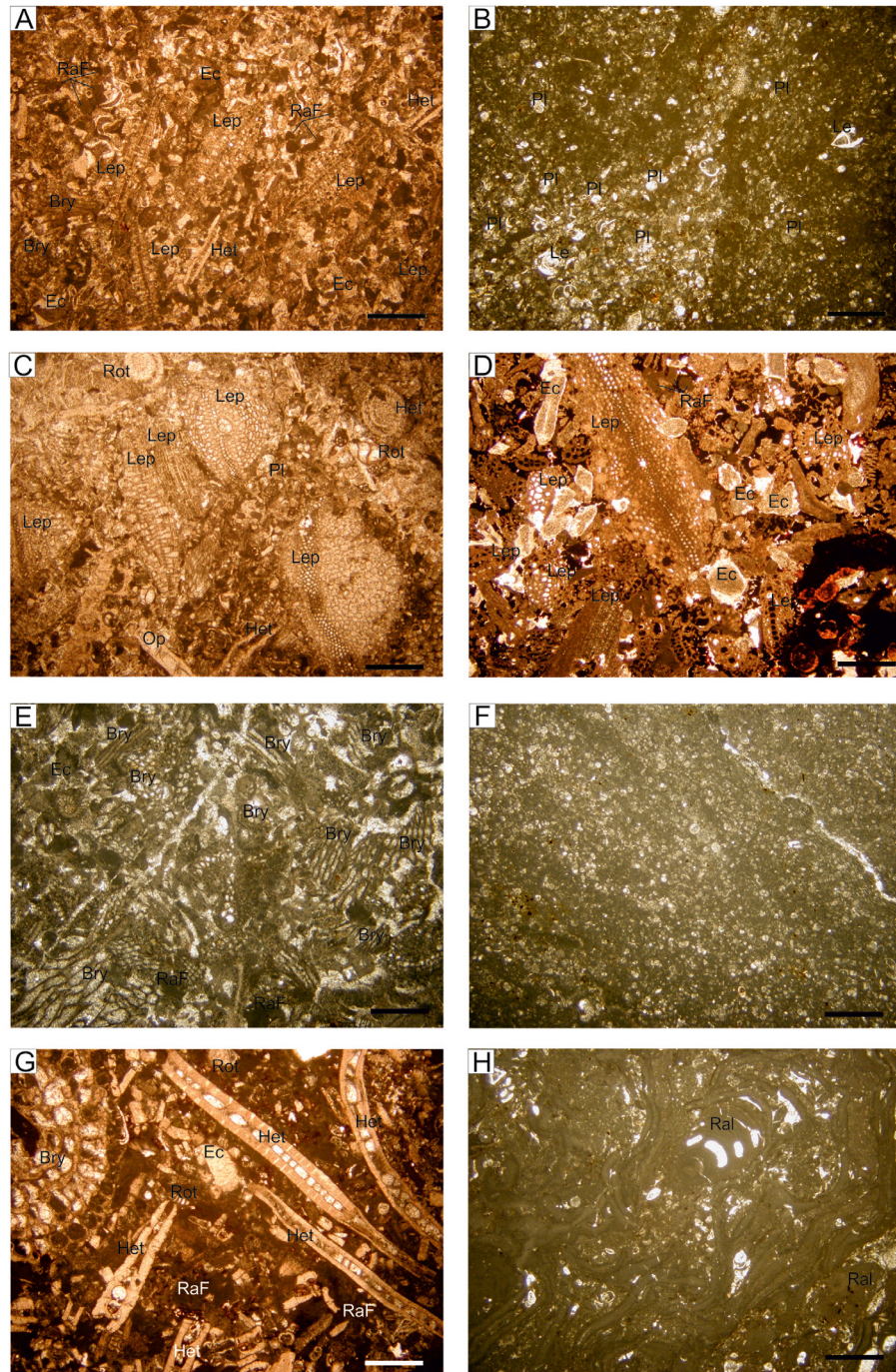


Fig. 4: Stratigraphic architecture of the Bolognano Formation with the measured stratigraphic sections (modified after Brandano et al., 2016a).



an environment colonised by seagrass meadows settled between the distal inner ramp and the middle ramp, whereas the distal portion of the middle ramp is characterized by a bioclastic packstone, together with red algal bindstone facies. The last and youngest unit of the Bolognano Fm is constituted by the *Turborotalita multiloba* marls, deposited in a hemipelagic setting during the end of the early Messinian. Above the *T. multiloba* marls, the evaporites of the Gessoso-Solfifera Fm have been deposited, recording the Messinian crisis of the Mediterranean (Crescenti et al.,

Fig. 5: Photomicrographs of the six units forming the Bolognano Fm. A) Thin section of *Lepidocyclina* Calcarenite 1 unit with lepidocyclinid specimens together with bryozoans and other fragmented bioclastic fraction represented by echinoids, red algal fragments and nummulitids (as *Heterostegina*). B) Cherty marly limestone unit rich in planktonic foraminifera and subordinated small benthic foraminifera as *Lenticulina*. C) *Lepidocyclina* Calcarenite 2 unit dominated by *Eulepidina* and *Nephrolepidina* specimens and subordinated nummulitid fragments, echinoids, rotaliids and rare planktonic foraminifera. D) *Lepidocyclina* Calcarenite 2 unit showing the bitumen shows characterizing this unit and infilling the intraparticle and interparticle porosity. E) Bryozoan calcarenite unit dominated by bryozoan colonies, red algal fragments and fragmented bioclasts. F) Hemipelagic marly limestone and calcareous marls unit with abundant planktonic foraminifera tests of orbulinids and globigerinids. G) *Heterostegina* level characterizing the base of the *Lithothamnion* unit of the Bolognano Fm. H) Thin section of the *Lithothamnion* limestone unit showing a melobesioid multi-layered encrusting thallus forming a rhodolith. For all the thin section the scale bar is 500µm. Lep = *Lepidocyclina*, Br = bryozoan, Ec = echinoid, Ro = rotaliid, Raf = red algal fragment, Het = *Heterostegina*, Op = *Operculina*, Pl = planktonic foraminifera, Le = *Lenticulina*.



1969). Lastly, during the early Pliocene, the Majella Mountain was involved in the foredeep system of the Apennine orogeny (Cosentino et al., 2010).

Early Miocene paleoceanographic setting

The Miocene was a crucial interval for the paleogeographic evolution of the Mediterranean area. During the early Miocene, the Mediterranean was connected to both the Indo-Pacific and the Atlantic Oceans (Popov et al., 2004; Rögl, 1999; Okay et al., 2013).

The collision between Arabia and the Eurasia plates closed the Neotethyan Oceanic Gateway by isolating the Mediterranean from the Indian Ocean during the middle Miocene (Okay et al., 2013). The disconnection of the Mediterranean area from the Indian Ocean resulted in the interruption of the low latitude circumglobal ocean circulation, blocking the exchange of surface and deep waters between the Indian and the Atlantic Oceans (de la Vara, A. & Meijer, 2016). Radiogenic Nd isotopes indicate a first reduction during the late Burdigalian (Rögl, 1999), and a final closure during the Langhian-Serravallian (Kocsis et al., 2008, Cornacchia et al., 2018). This evolution of the Indo-Pacific connection strongly influenced the Mediterranean circulation, and different models of circulation and exchange with the adjacent oceans have been proposed (Karami et al., 2009; de la Vara et al., 2013; de la Vara and Meijer, 2016).

According to de la Vara et al. (2013), a deeper Indian Gateway promoted in the Mediterranean an anti-estuarine exchange with both adjacent oceans, with a westward surface flow from the Indian Ocean and an eastward flow at depth. Successively, when the depth of the Indian Gateway significantly reduced during late Burdigalian (Okay et al., 2013), an estuarine circulation was promoted and persisted during the Langhian favored by more humid and warmer climate (Gebhardt, 1999; Dell'Antonia, 2003; Bohme et al., 2011, de la Vara and Meijer, 2016). In this scenario, the Indian Ocean's shallow-water overlapped those of the Mediterranean, moving westward and flowing into the Atlantic (De la Vara and Meijer, 2016). Consequently the Indian Gateway can be considered closed from a paleoceanographic perspective. Nevertheless, the Nd isotope signatures of Mediterranean water masses indicate an unequivocal contribution of Indian Ocean waters lasting until the Serravallian (Kocsis et al., 2008; Cornacchia et al., 2018), thus a persistent westward flow from the Indian Ocean has to be considered. According to the Mediterranean paleogeographic reconstruction (Fig. 6), the surface waters flowed westward and northward in the proto-Adriatic Sea, a basin about 800 - 1000 km wide in the Western Mediterranean. Within this basin, two carbonate platforms, the Latium-Abruzzi and Apulia, persisted separated by the Genzana



basin connected southward with the Molise Basin.

Within this mosaic, phosphate hardgrounds may provide additional insight in the reconstruction of the deep currents as they are thought to be the product of upwelling and deep nutrient-enriched currents (Burnett et al., 1983; Föllmi, 1996; Föllmi et al., 2008; 2015; Vescogni et al., 2018; Brandano et al., 2016b; 2020). Lower Miocene phosphate rich intervals occur in Malta and Sicily (Pedley and Bennet, 1985; Föllmi et al., 2008), and in the Majella (Mutti and Bernoulli, 2003).

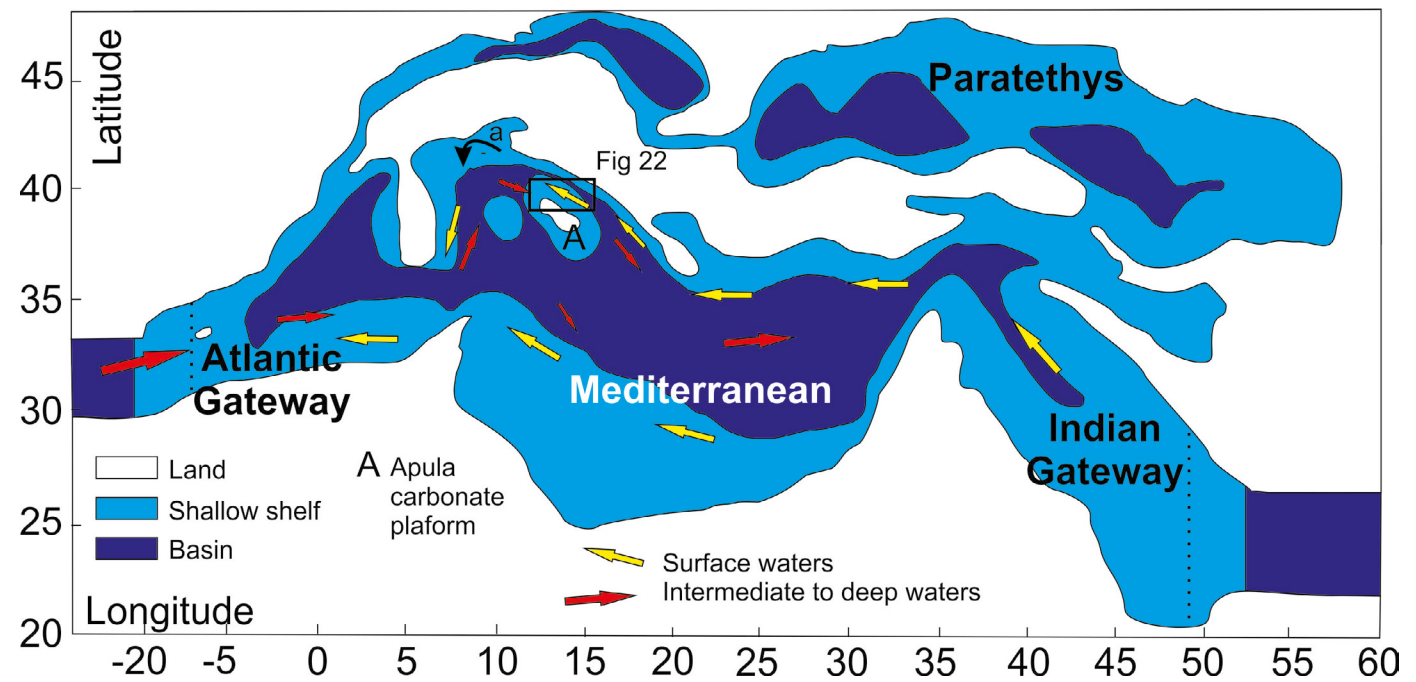


Fig. 6: Paleogeography of the Mediterranean area during Burdigalian.

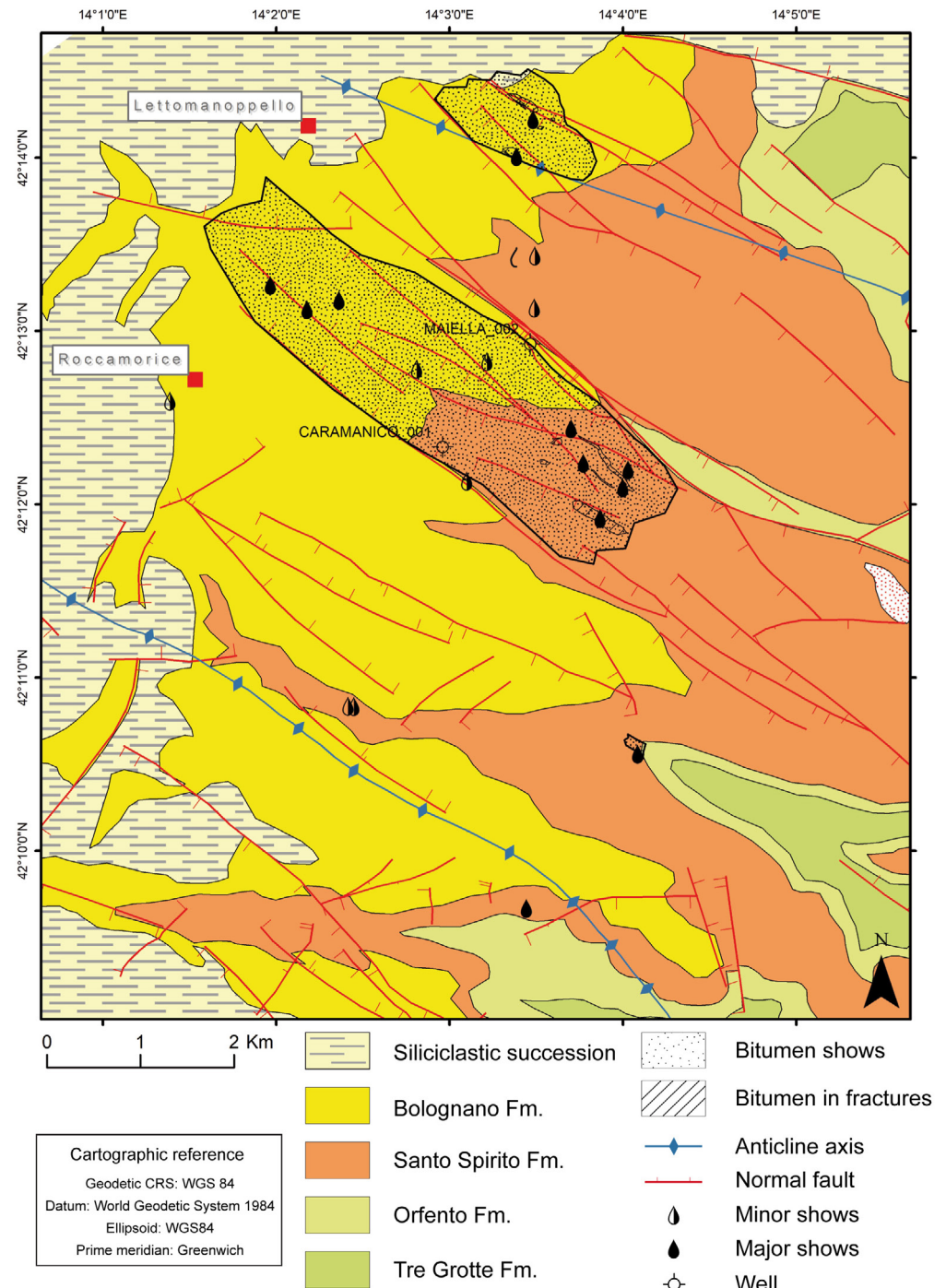
Oil shows and Bitumens in the Majella Area

During the second half of the XIX century the Majella area represented the vanguard of the Italian oil industry (Jervis, 1873; Magini, 1977; Novelli and Sella, 2009; Gerali and Lipparini, 2018). Moreover, this area has been severely exploited during the early twentieth century, being at that time, the second-largest oil district in Italy after the Emilia Romagna region (Gerali, 2013). From the petroleum system point of view, the Northern sector of the Majella Mountain presents all the needed elements: the source is represented by the Late Triassic-Early Liassic carbonates/evaporites (Cazzini et al., 2015); the reservoir is mainly represented by the carbonate-ramp sequence developed over the Cretaceous platform and its slope (Agosta et al., 2010; Brandano et al., 2013; Scrocca et al., 2013; Lipparini et al., 2018); the seal is represented by both marly levels within the Bolognano Fm (Brandano et al., 2013; Lipparini et al., 2018; Trippetta et al., 2020) and by the Messinian Evaporites (Iadanza et al., 2015) whereas overburden rocks are represented by the overlying younger formations.

In the whole NW sector of the Majella massif, several near-surface and outcropping reservoirs are found locally filled with hydrocarbons at different stratigraphic levels such as the Bolognano Fm reservoirs (Oligocene–Miocene; Scrocca et al., 2013), and also within the carbonates of the Santo Spirito (Paleocene–Oligocene) and Orfento (Upper Cretaceous) Fms. Hydrocarbons, mainly as bitumen, saturates both the rock's matrix and fractures, in particular within the high-porosity carbonates of the Bolognano Fm (Vecsei and Sanders, 1999). Moreover, further to the North, the same saturated reservoir rock (on average at less than 1 km depth) has been greatly investigated and exploited, within the Vallecupa and Cigno oil fields (ViDEPI Project, 2012).

Different interpretations for the oil distribution over the whole NW sector of the Majella area have been proposed in the literature. Based on the structural interpretation of the northern Majella Mountain and the fault architectures, Agosta et al. (2009) suggested that the major faults formed the prime pathways to subsurface fluid flow, assessing that hydrocarbons were channeled along these faults at certain depths, then migrated upward mainly within the deformed carbonates at the extensional jogs of interacting oblique

Fig. 7: Simplified geological map showing the distribution of bitumens and the location of the two exploration wells drilled in the study area (modified from Vezzani and Ghisetti, 1998 and Brandano et al., 2013).





normal faults. Lipparini et al. (2018), however, by means of a dataset of shallow wells drilled in two areas, observed that most of the faults do not influence significantly the hydrocarbon presence and its saturation, suggesting for this area a minor role of faults in the hydrocarbon migration.

From a purely geometrical point of view, the hydrocarbon distribution over the area follows an almost NW–SE-oriented trend (Fig. 7), in accordance with the NW–SE-dominating fault trend observed nowadays in the outcrops (e.g. Vezzani and Ghisetti, 1998). This can be related to the capacity of a major NW–SE fault to limit the extension of hydrocarbon occurrence, as suggested by the Piano delle Cappelle main fault. This fault appears today as a sealing fault, related to either the lateral juxtaposition of low-porosity units caused by the large displacement (ca. 180 m), or the possible sealing properties of the fault core, as confirmed by the absence of oil within the cemented fault-breccia.



DAY 1

On this day, we will focus on the general stratigraphic and tectonic setting of the Majella Mountain from the Blockhaus panoramic point (Fig. 1). Successively, we will analyse the stratigraphic architecture of the Bolognano carbonate ramp (Fig. 4). Starting from the north-western sectors, in particular in the Orfento valley, we will then cross the S. Bartolomeo valley to arrive in the eastern sectors, which will be analysed during the second day of the field trip. In the Orfento Valley, we will observe the detail of the stratigraphic succession in the Decontra section, while in the panoramic view of the area between the Giumentina and the S. Bartolomeo Valleys it will be possible to observe the vertical and lateral changes of the Bolognano Fm lithostratigraphic units, which correspond to the environmental and climatic changes occurred between the late Oligocene and the middle Miocene.

Stop T6.1.1

Panoramic view of Majella Carbonate Platform from Blockhaus and Monte Cavallo (42°08'42.21''N, 14°06'39.76''E)

The panoramic view from Blockhaus allows recognizing the main stratigraphic architecture of the platform and the transition to the adjacent basin (Fig. 8). The platform can be subdivided into a Lower Cretaceous portion (Monte Pacentro Fm) separated from the Upper Cretaceous portion (Cima delle Murelle Fm) by an unconformity evidenced by karst features and bauxite deposits, ranging from late Albian to early Cenomanian in age (Vecsei et al., 1998). This unconformity is associated with a 5° tilt that can be related to the onset of the extensional tectonic activity in the Late Cretaceous in this part of the Adriatic plate (Vitale et al., 2017; Eberli et al., 2019). Another exposure of the platform occurred during the early to middle Campanian, and concluded the shallow-water platform aggradation phase. The platform margin is cut by a steep and incised escarpment. This escarpment displays a scalloped geometry indicating significant sub-marine erosional processes occurring during platform margin growth. The margin was also segmented along strike orientation and characterised by highs and lows. The depression next to the Monte Rotondo corresponds to the 'drowning seaway' of Rusciadelli et al. (2003) and to the 'Rotondo Channel' of Eberli et al. (2019). The escarpment is overlapped in the lower part by redeposited bioclastic calcarenites of Valle dell'Inferno unit (Cenomanian) and by magabreccias, bioclastic calcarenites and pelagic limestones of Tre Grotte Fm (Turonian to early Campanian). This onlap is spectacularly visible in the upper part of Valle dell'Orfento from the Monte Cavallo panoramic point. During the Campanian-Maastrichtian, the calcarenites

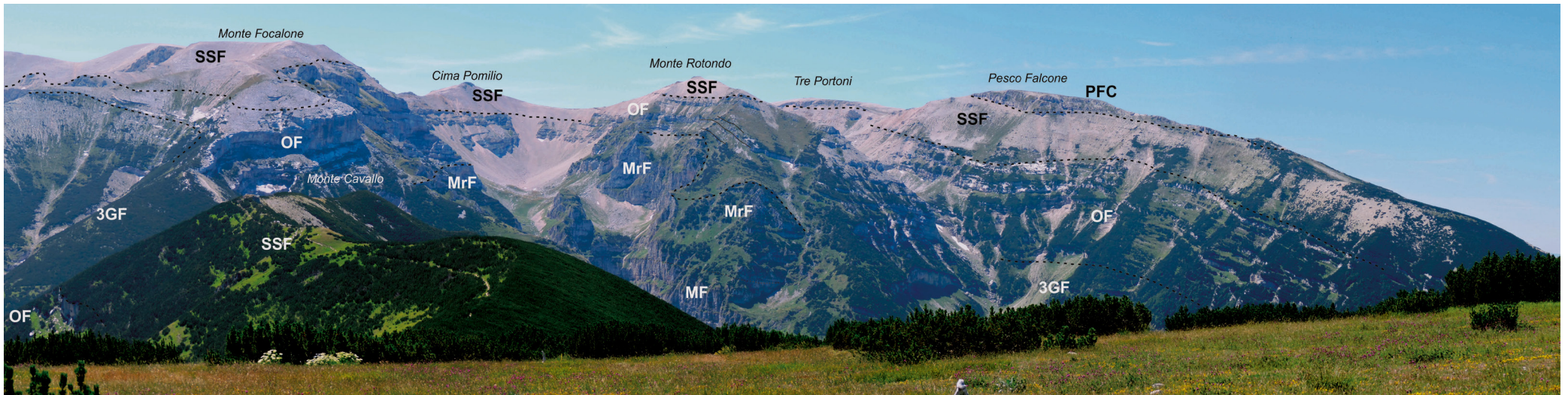


Fig. 8: Panoramic view of the Majella stratigraphic architecture from the Blockhaus, MF = Morrone Fm (Late Jurassic – Early Cretaceous), MrF = Cima delle Murelle Fm. (early Cenomanian–late Campanian), 3GF = Tre Grotte Fm (late Turonian–late Campanian), OF = Orfento Fm (late Campanian–Maastrichtian), SSF = Santo Spirito Fm (Danian–Rupelian), PFC = Pesco Falcone Coral clusters (Rupelian).

of the Orfento Fm prograded over the former basin filled by resedimented sediments shed by the platform since the Turonian until the beginning of the Campanian. The progradation is well observable along the slope of Monte Falcone. The Monte Cavallo point offers a beautiful view of the wedge-shaped geometry of the Orfento Fm delta drift *sensu* Eberli et al. (2019; Fig. 8). The overlying deposits of the S. Spirito Fm (Danian–Bartonian) consist of outer ramp lithofacies represented by a bioturbated, fine, planktonic-rich packstone to wackestone, a bioclastic floatstone alternating with breccias and a bioclastic floatstone to rudstone rich in larger benthic foraminifera. Another unconformity, once again produced by the emersion of the platform, marks the contact between the S. Spirito Fm and the large coral mounds of the Monte Pesco Falcone Fm (Vecsei et al., 1998, Vecsei and Sanders, 1997; Brandano et al., 2019). This unconformity represents the sedimentary record of the sea-level drop of several tens of meters occurred during the Eocene to Oligocene transition (Brandano et al., 2019). The coral bioconstructions developed in a middle ramp environment where luxurious corals built up discrete structures as mounded cluster reefs (Fig. 8). The coral bioconstructions grew seaward of the euphotic seagrass zone. During sea-level rises and following highstands, the cluster reefs coalesced to form an extensive coral unit that prograded for some kilometers toward the basin and interfingered with the outer ramp deposits (Brandano et al., 2019).

Stop T6.1.2

Valle dell'Orfento, the Decontra stratigraphic sections (42°09'46.78"N; 14°02'21.80"E)

The Decontra stratigraphic section is observable in the upper part of Orfento Valley, along the path from Decontra village to Serra S. Antonio (Fig. 9). The base of the section consists of 32 m of the first stratigraphic unit, the

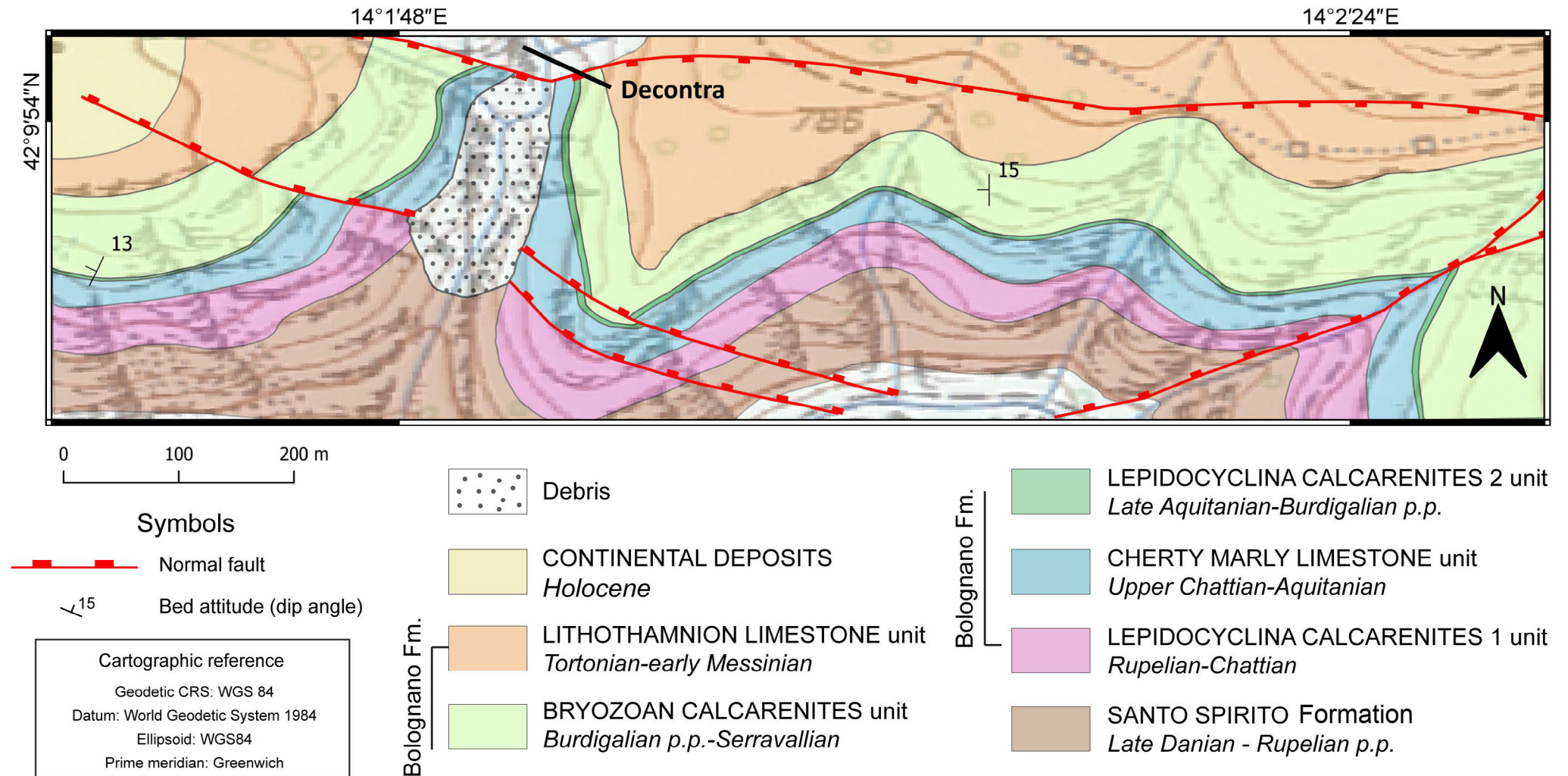


Fig. 9: Geological map of Decontra area.



Lepidocyclina Calcarenite 1 (Figs. 10, 11). This unit is mostly represented by cross-bedded calcarenites consisting of grainstones to packstones with larger benthic foraminifers (LBF) (Fig. 5A, C, D). The main components are in fact *Nephrolepidina*, *Eulepidina*, *Heterostegina* and *Operculina*. Other common components are small benthic foraminifers (SBF) such as rotaliids, *Rotalia*, *Neorotalia viennoti*, *Lobatula lobatula*, *Lenticulina*, *Planorbulina*, discorbaceans, buliminaceans, textularids, and rare miliolids. Red algal debris and bryozoan fragments are frequent, while minor components are *Ditrupa*, echinoid and bivalve fragments and planktonic foraminifera. Two main types of cross-bedding can be recognised in this unit, planar cross-bedding and cuneiform to sigmoidal-shaped cross-bedding (Brandano et al., 2012). LBF biostratigraphy allowed to ascribe this unit at the SBZ22a of Cahuzac and Poignant (1997), therefore to the Rupelian-Chattian stratigraphic interval (Benedetti et al., 2010). The *Lepidocyclina* Calcarenite 1 are overlain by 23.5 m of the cherty bioturbated packstone to wackestone, and nodular bioclastic wackestone to packstone with SBF and bryozoan fragments. Glauconite is common. Age constraints are provided by calcareous nannofossil biostratigraphy. The base of the cherty marly limestones has been attributed to the upper Chattian while the top of the unit is the upper Aquitanian (Brandano et al., 2016a). The Cherty marly limestones are overlain by the *Lepidocyclina* Calcarenite 2, which

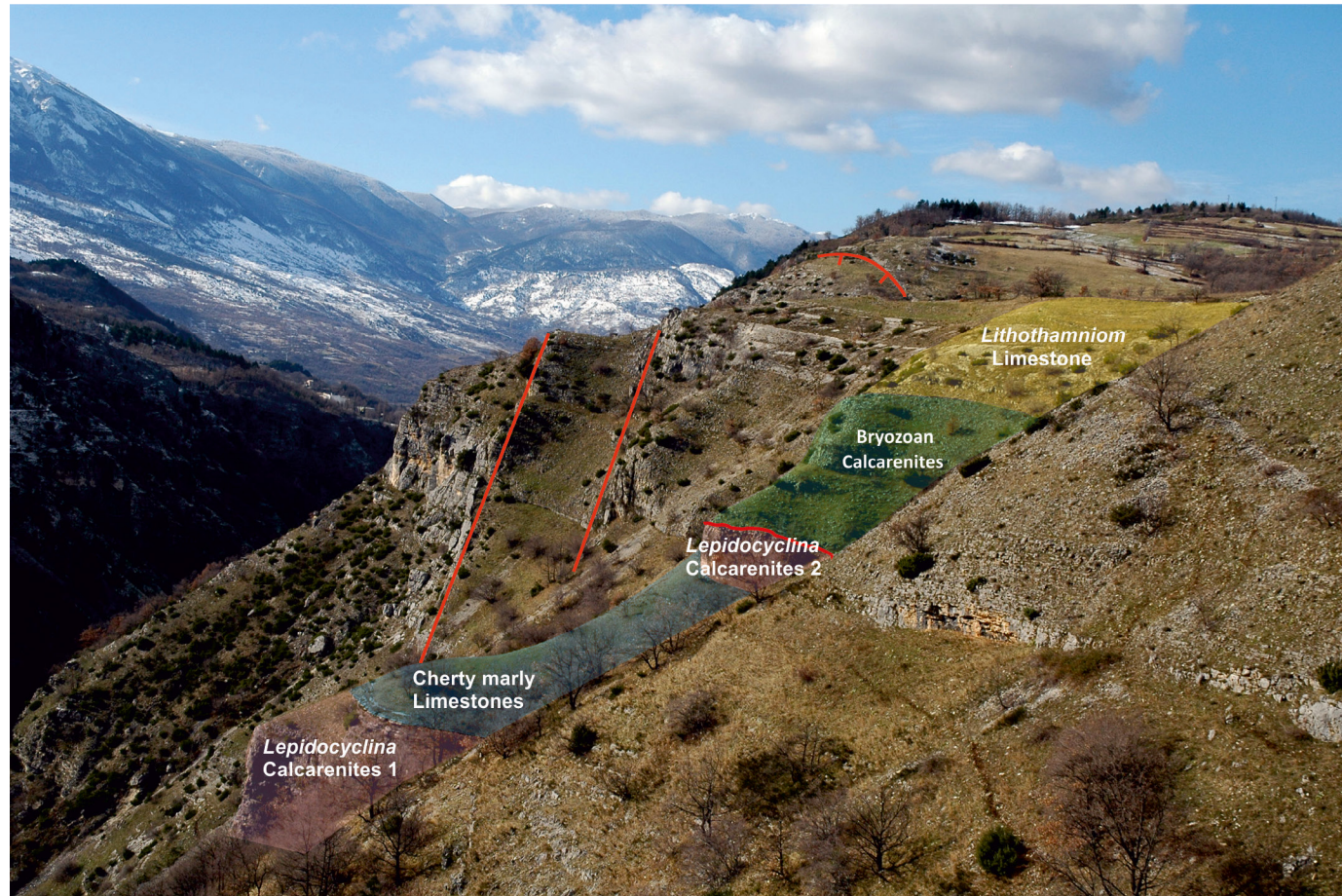


Fig. 10: Panoramic view of Decontra stratigraphic section with photomapping of the main lithostratigraphic units of Bolognano Fm cropping out in the Orfento Valley.

is overlain by 23.5 m of the cherty bioturbated packstone to wackestone, and nodular bioclastic wackestone to packstone with SBF and bryozoan fragments. Glauconite is common. Age constraints are provided by calcareous nannofossil biostratigraphy. The base of the cherty marly limestones has been attributed to the upper Chattian while the top of the unit is the upper Aquitanian (Brandano et al., 2016a). The Cherty marly limestones are overlain by the *Lepidocyclina* Calcarenite 2, which



are strongly reduced in the Orfento Valley, they are in fact only 2 m thick and are represented by a bryozoan floatstone. A phosphatic hardground, identified over the entire Bolognano ramp, marks the drowning of the *Lepidocyclina* Calcarenite 2 (Mutti and Bernoulli, 2003). Above the hardground, 28 m of bryozoan calcarenites lie. These calcarenites consist of bioclastic packstones dominated by bryozoan and echinoid fragments (Fig. 5E, Fig. 11). This lithofacies is characterized by planar to trough cross-bedding. The beds are 0.2 to 0.6 m thick and they are separated by marly layers of few cm in thickness. The overlying unit, the *Lithothamnion* limestone, lies unconformably on the Bryozoan calcarenites. The base of this unit is marked by a 1.5 m thick *Heterostegina* level (Fig. 5G), followed upward by 33.5 m of thick-bedded red algae packstones and free living red algae rudstones to floatstones (Fig. 5H). The skeletal assemblages are dominated by larger benthic foraminifers (*Amphistegina*, *Operculina* and *Heterostegina*), smaller benthic foraminifers (*Elphidium*, rotalids), bryozoans, bivalve fragments, vermetid tubes, and echinoid fragments. Three different stages in the evolution of this unit can be recognized. During the first stage, the ramp was subjected to high-energy wave-dominated conditions. In the second stage, coralline algal (mäerl) facies and seagrass meadows developed, initially in an oligotrophic setting, later followed by a slight reduction in light penetration. The third stage involved a general increase in fine terrigenous sediments, together with a further decrease in light and also by the spread of coralline algal bindstone facies. The elevated terrigenous input was associated with increased trophic conditions, as also shown by the occurrence of abundant plankton and low-oxygenated foraminiferal assemblages (Brandano et al., 2016c). The base of the *Lithothamnion*

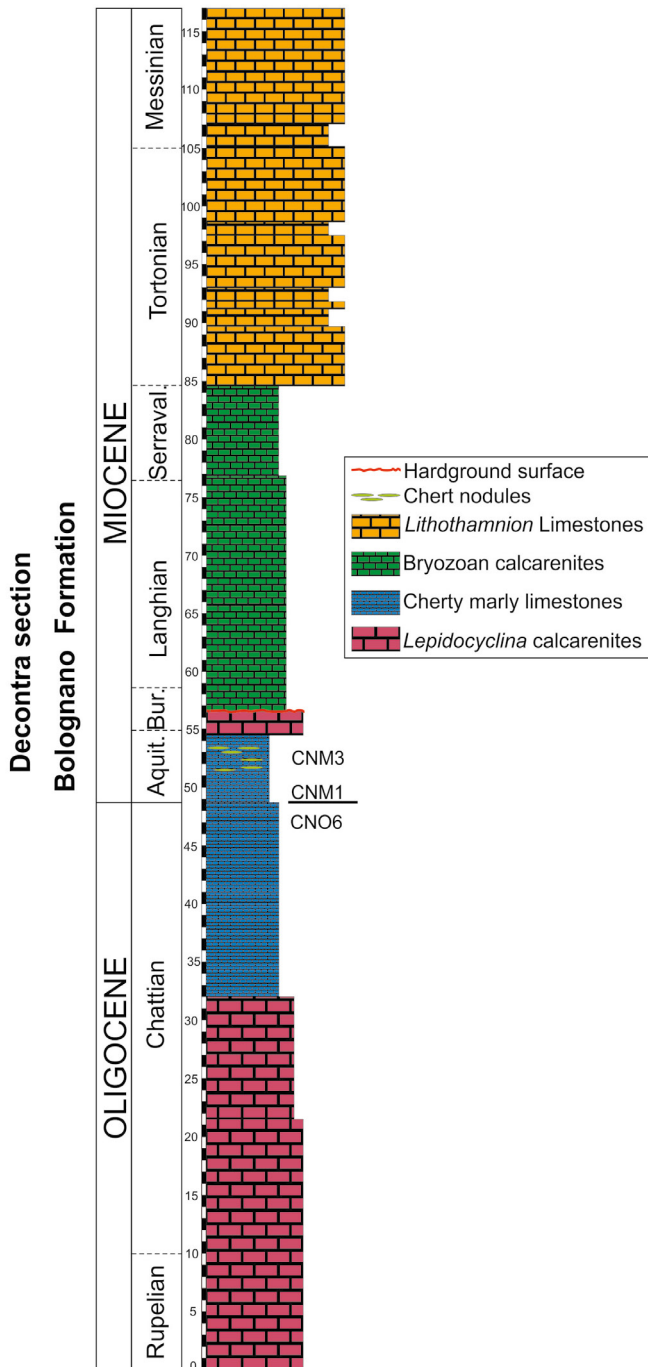


Fig. 11: Stratigraphic log of Deontra section and chronostratigraphy and lithostratigraphy of Bolognano Fm (after Brandano et al., 2016a).



limestones has been ascribed to the Tortonian by means of Sr Isotope stratigraphy, while the upper portion of this unit is Messinian in age due to the occurrence of the small benthic foraminifer marker *Bulimina echinata* (Patacca et al., 2008; Cornacchia et al., 2017).

Stop T6.1.3

Panoramic view of S. Bartolomeo Valley (42°10'52.70"N; 14°02'05.61"E)

The panoramic view from the southern side of S. Bartolomeo Valley provides a spectacular view of the Bolognano Fm stratigraphic architecture (Fig. 12). The view shows two calcareous lithostratigraphic units separated by a marly unit (Fig. 13). The debris of the marly unit result in scree-producing elements, while the limestones of the *Lepidocyclina* units form weather resistant cliffs. The basal unit is represented by *Lepidocyclina* Calcarenites 1 that overlies the Eocene carbonates of the S. Spirito Fm. Here the thickness of this unit is 53 m. The

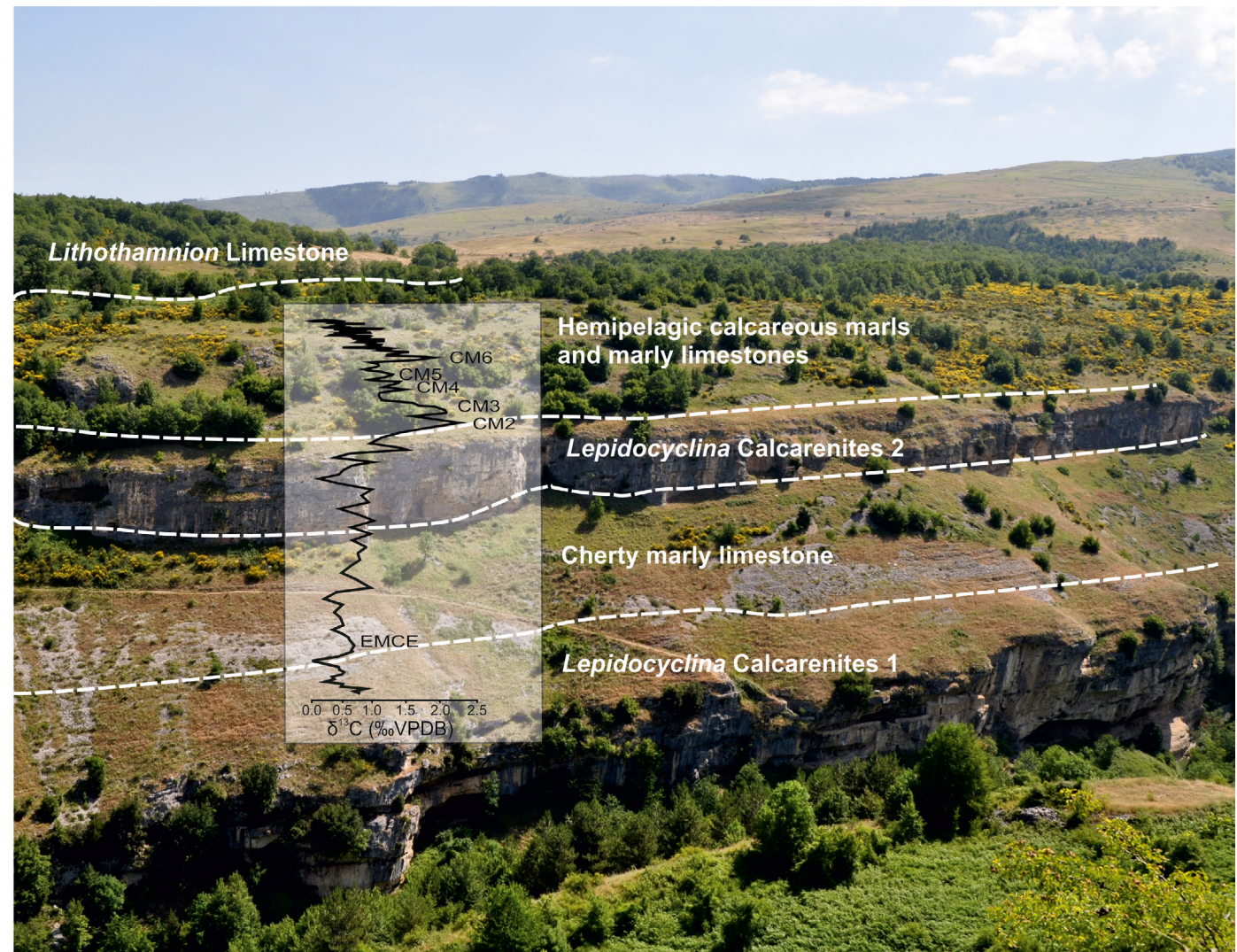
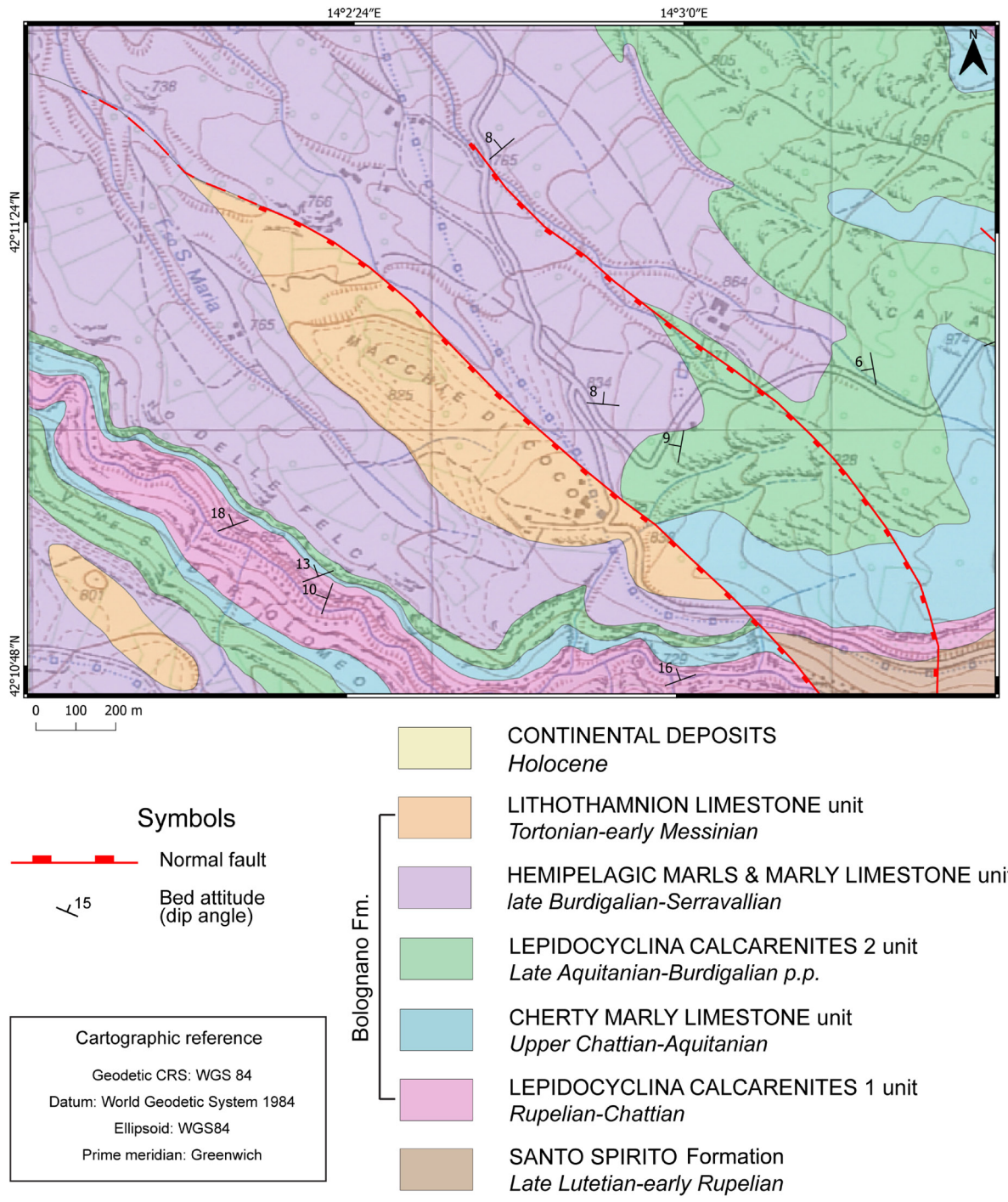


Fig. 12: Panoramic view of the S. Bartolomeo Valley with photomapping of the main lithostratigraphic units of the Bolognano Fm and the relative C-isotope curve from Brandano et al. (2017).



Lepidocyclina Calcarenite 1 are overlain by the cherty marly limestone unit, 18 m thick, overlain by another cross-bedded calcarenites unit, the *Lepidocyclina* calcarenites 2. The *Lepidocyclina* Calcarenite 2 unit shows compositional and sedimentological characteristics that are similar to those of the basal *Lepidocyclina* Calcarenite 1 unit, except for a decrease in abundance of larger benthic foraminifer specimens. The thickness of this unit in the S. Bartolomeo valley increases up to 16 m with respect to Orfento valley where it was only 2 m thick. In the S. Bartolomeo valley, the *Lepidocyclina* Calcarenite 2 is overlaid by the hemipelagic marls unit instead of the bryozoan calcarenites observed in the Orfento valley (Figs. 4, 9).

In this area, the basal portion of the composite S. Bartolomeo Valley–Orta stratigraphic section has been measured and sampled. This section records the Chattian–Serravallian evolution of the Bolognana Fm. In particular, the section displays a good record of the EMCM (Early Miocene Carbon Maximum) and the Monterey Excursion (Fig. 12). In fact, the carbon isotope record is marked by a minor, but sharp, positive $\delta^{13}\text{C}$ shift at the Oligocene-Miocene boundary. This isotopic

Fig. 13: Geological map of S. Bartolomeo area.



shift corresponds to the drowning of the *Lepidocyclina* Calcarenite 1 carbonate ramp, overlain by the Cherty Marly Limestone unit. The increase in $\delta^{13}\text{C}$ values reflects an increased productivity of surface seawater. Eutrophic events may have caused the drowning of carbonate platforms due to the shift from photo-dependent-dominated to the filter feeding biota (Mutti and Hallock, 2003). The onset of the Monterey Event in the Bolognano Fm is recorded by the *Lepidocyclina* Calcarenite 2 unit, which is characterized by the abundance of bryozoans and echinoid fragments in place of larger benthic foraminifera. The spread of bryozoans has been linked to an increased nutrient availability in surface waters (Brandano et al., 2010; 2017). Under an enhanced nutrient flux, due to continental runoff or upwelling, phytoplankton blooms may increase the surface water turbidity, thus reducing the light available for the bottom-dwelling organisms, such as the larger benthic foraminifera.

DAY 2

The second day will be focused on the large dune field characterizing the *Lepidocyclina* Calcarenite 2 in the outcrop of Piano delle Cappelle. In the last stops of the field trip we will observe as this unit represents an exhumed part of a petroleum system that was active in the northern part of Majella area. Hydrocarbon occurrences in both matrix and fracture porosity will be observed in detail in the stops of the Acquafredda block and in the Valle Romana Quarry, where beautiful exposure of bitumen shows and seepages are present.

Stop T6.2.1

Piano delle Cappelle – Dune field (42°13'00.21"N; 14°04'18.17"E)

The Piano delle Cappelle area is dominated by *Lepidocyclina* Calcarenite 2 (Fig. 14). Along the road leading to the abandoned S. Maria quarry, it is possible to analyse the spectacular sedimentary structures characterizing this unit. The *Lepidocyclina* Calcarenite 2 represents the sedimentation between the oligophotic and the aphotic zone of a carbonate ramp environment affected by high energy currents. The sediment consists mainly of bryozoan colonies (celleporids and adeoniforms) and echinoids. Large benthic foraminifera are common and represented by *Nephrolepidina*, *Amphistegina* and nummulitids. Other minor components are red-algal debris, small benthic foraminifera, serpulid fragments, pectinid fragments, and planktonic foraminifera (Fig. 5A, C, D).

The cross bedding characterizing this unit is produced by the migration of submarine dunes (Fig. 15). In the initial part of the S. Maria Quarry road, the dunes correspond to a more distal sector of the ramp. Here



the palaeocurrent patterns are indicative of a generally basinward, north-west directed flow (Fig. 15A, 16). The dunes show dip azimuth in the range of 290°-320°. The geometries are typical of simple dunes without internal angular discontinuities and compound dunes with one order of discontinuity or, more rarely, two orders in internal organization. The first order sets contain parallel lamination. Foresets are generally tangential, with dip angles decreasing from 20° to few degrees toward the bottomset. Three-dimensional reconstructions of the bedforms were obtained by means of a terrestrial laser scanner (Brandano et al., 2012). The dunes generally show a planar lower bounding-surface shape, with dunes migrating on a flat surface. The height of the dunes ranges from 5 to 9 m, and their average length ranges from about 200 to 300 m. They have

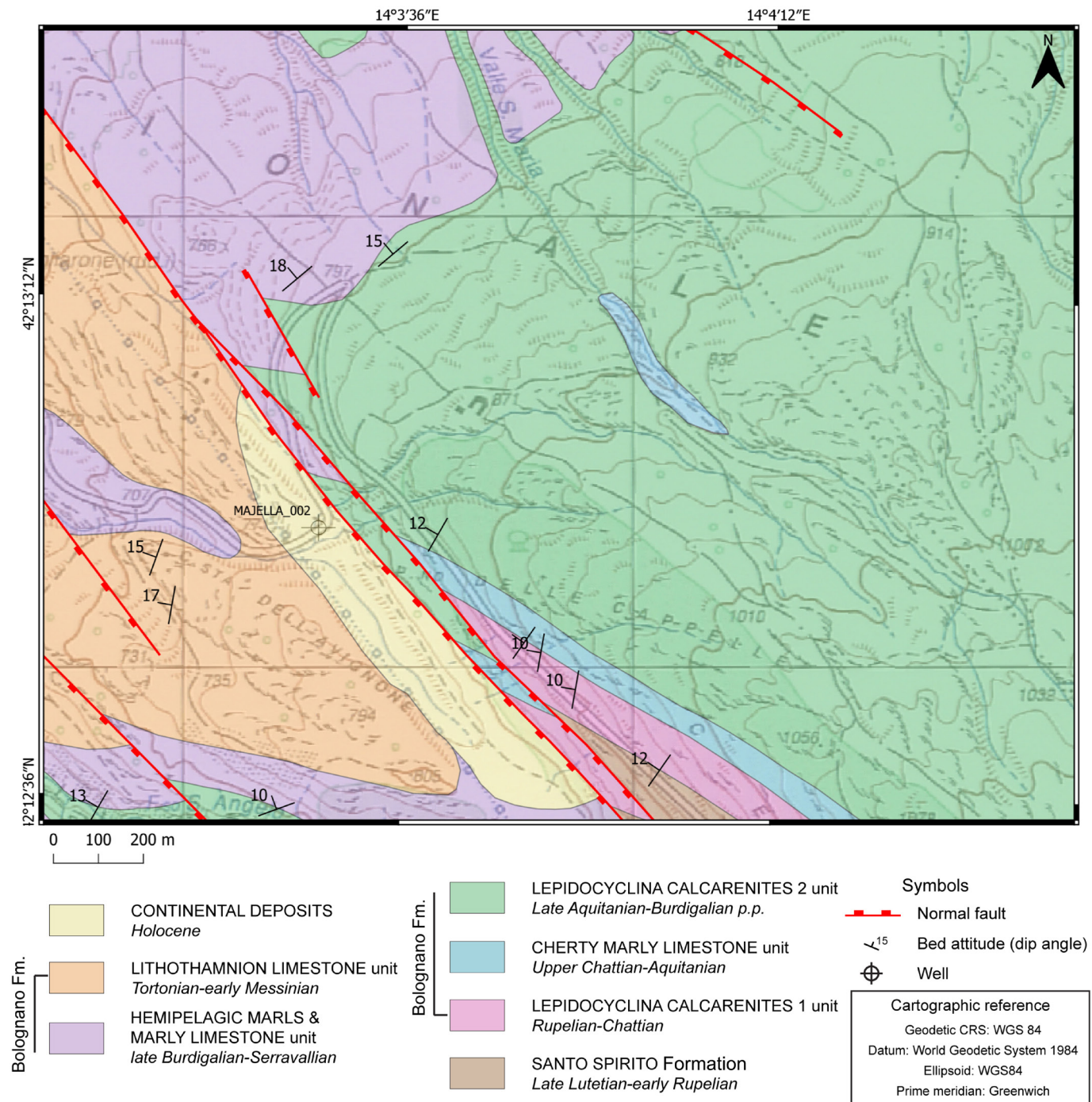
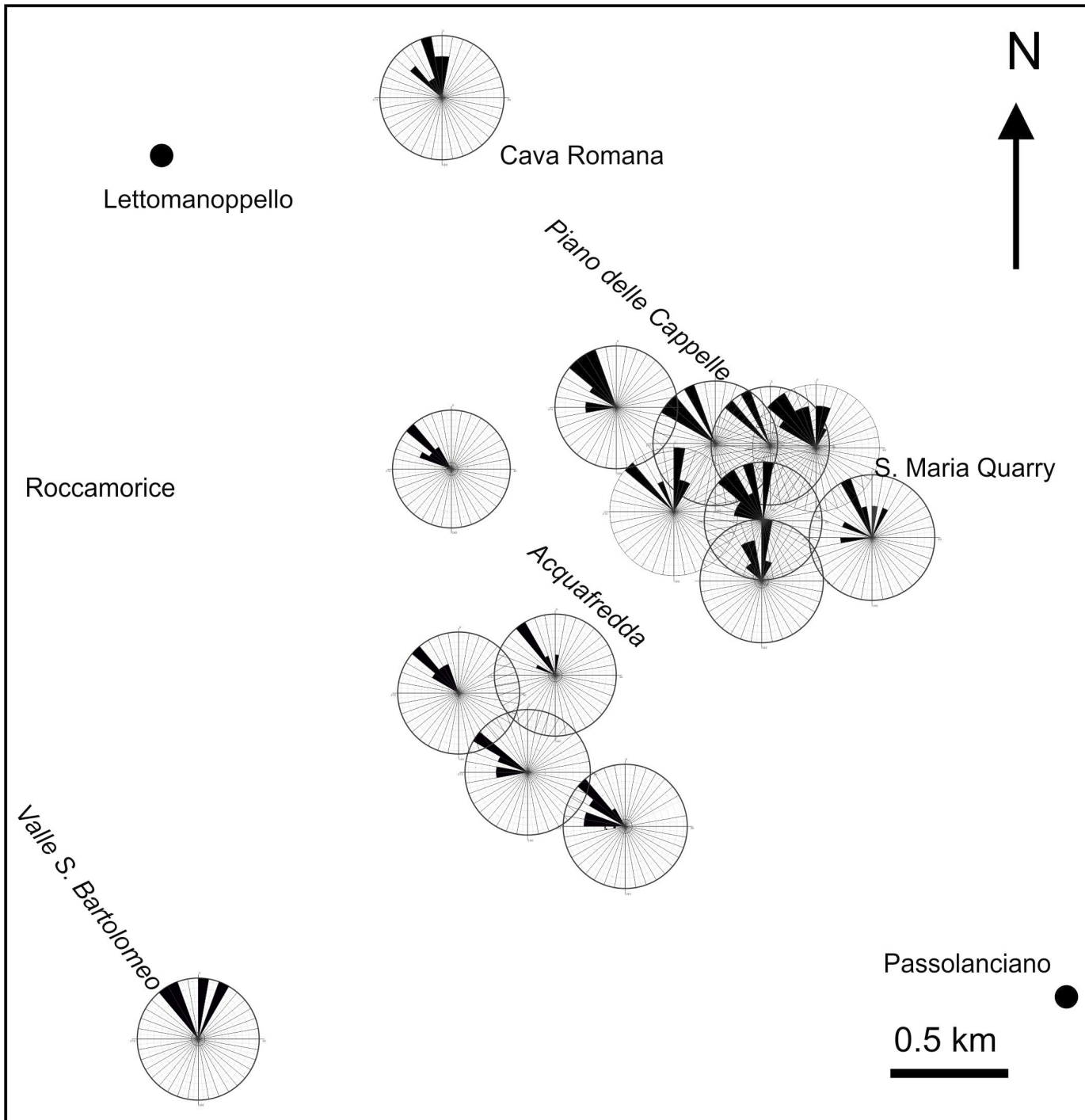


Fig. 14: Geological map of the Piano delle Cappelle area.



Fig. 15: cross-bedding of *Lepidocyclina* Calcarenite 2, A) northwest oriented simple and compound dunes bounded by flat surfaces; B) second order sets of a northeast oriented dune; C) interfingering of northwest and northeast oriented dunes.



straight or slightly sinuous crests, being considered mainly as 2D and subordinately 3D bedforms (*sensu* Ashley, 1990).

Walking 0.5 km toward the S. Maria quarry, we move toward more proximal environment of the middle ramp. Here the dunes show two main orientations (Fig. 16). A group is still oriented basinward with dip generally toward WNW and they display similar characters to the dunes previously described, the only difference is a reduced height of the composite dunes, up to 3-4 m. A second group of bedforms is perpendicularly oriented with respect the first group (Figs. 15B, C). The dip is generally toward NE of 20° and 10°. The sets are characterized by bedding-parallel lamination, the thickness ranges between 10 and 60 cm. These dunes show a trough-shaped bounding-surfaces, however flat

Fig. 16: Palaeocurrents in the *Lepidocyclina* Calcarenite 2. The generalized regional palaeocurrent direction is toward NW.



bounding surface may occur. The second order sets are up to 2 m thick and represent the stacking of 3D dunes one over the other, forming compound sets and compound dunes with slightly sinuous crests.

Stop T.6.2.2

Acquafredda Mines (42°12'14.08"N; 14°03'49.24"E)

The areal distribution and the characteristics of bitumen seeps within the *Lepidocyclina* Calcarenites 2 can be estimated at this stop (Fig. 18).

The stop starts very close to the point where the Caramanico 1 well has been drilled in the 1976, reaching a total depth of 5540 m (Fig. 7, 17). The main target of this perforation was the supposed source rock represented by the Triassic Evaporites (Cazzini et al., 2015). This formation has been encountered from ~2850 m down to the total depth of the well, however, the Triassic Evaporites do not show evidences of activity as a source rock.

In the past, the Acquafredda area was one of the main sources for bitumen extraction, as it is possible to appreciate by looking at the abandoned mines (tunnels and trenches) that are widespread on this area. The shallow extraction activity deeply modified the topography, as shown by the several debris of the ancient extraction activity visible by walking toward the Colle dell'Astoro, (Fig. 18A). Such debris were heated in the furnaces to obtain asphalts ready to be sold. The intense activity is the main proof of the large amount of bitumen that was and still is permeating the Bolognano Fm in this area.

Two main NW-SE trending faults border the Acquafredda mines whilst in the middle of the area no major faults have been ever reported, nor they are currently observable in the field. However, the absence of large faults

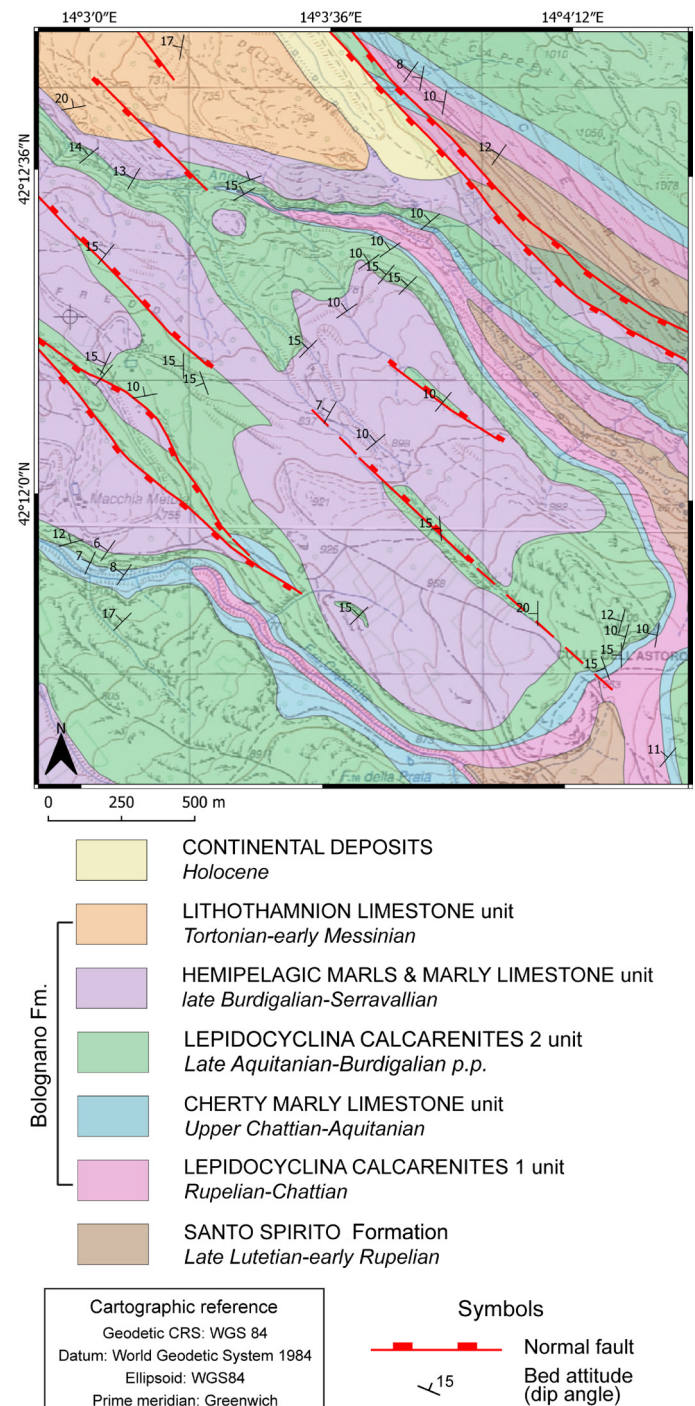


Fig. 17: Geological map of Acquafredda area.

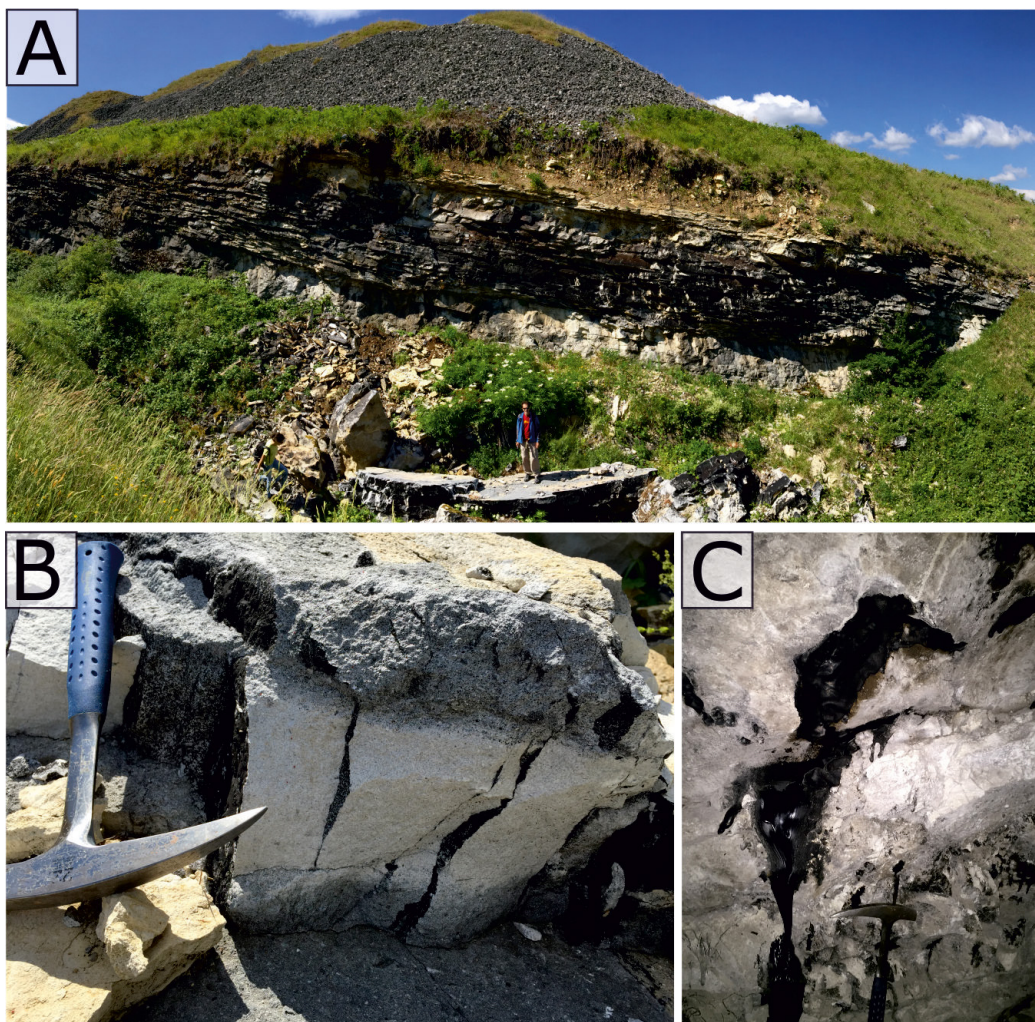


Fig. 18: Acquafredda mines, A) panoramic view of a trench within saturated *Lepidocyclina* Calcarenites 2. Note on top the debris resulted from the extraction activity. B) Detail of the saturated *Lepidocyclina* Calcarenites 2. Hydrocarbon saturation is evident close to the stratabound and within fracture planes. C) Bitumen that naturally flows out from a fracture in a mine tunnel.

nearby allows analyzing the fracture distribution in a homogeneous dataset not influenced by the presence of damaged zones. In a recent work (Trippetta et al., 2020), scanlines have been analyzed in order to investigate the role of fracture in the hydrocarbon circulation. Results show that fractures for both HHC-bearing and clean outcrops are mainly of the same type (joints-type with aperture not more than 2mm with few stylolites and very few small faults, Fig. 18A, B) and are characterized by the same orientation (NW-SE and NNE-SSW) in agreement with literature data on the Bolognano Fm (Di Cuia et al., 2009) and on older formations (Lavenu et al., 2014). The main difference between the two types of outcrops (clean and hydrocarbon-bearing) is that the absolute number of measured fractures is four times lower in hydrocarbon-bearing outcrops with respect to clean outcrops. It is also worth noting that the Colle dell'Astoro outcrop, located uphill along the Acquafredda path, shows higher fracture density (Trippetta et al., 2020) and it is free of hydrocarbon (Scrocca et al., 2013). This boundary has been proposed as the old oil-water contact (OWC) of this reservoir by Scrocca et al. (2013), while the difference in fracture density has been interpreted as a consequence of the different mechanical behaviour of hydrocarbon-saturated and clean rocks. Moreover, matrix saturation seems to be parallel to the bedding and thus not influenced by the orientation of fractures (Fig. 18B). On the other hand, fractures surely act as a drainage surface due to the



increased permeability parallel to the fracture plane as frequently observed in the field (Fig. 18C). Trippetta et al. (2020) interpret this as an evidence of the fact that, when the last stage of fracturing occurred in this area, hydrocarbons were already in place. In this view, hydrocarbons flowed toward the newly formed fractures from an already saturated matrix, and the presence of hydrocarbons limited the formation of fractures with respect to clean rocks.

Stop T6.2.3

Valle Romana Quarry (42°14'23.73"N; 14°03'26.00"E)

The ancient Valle Romana bitumen quarry, exploited since Roman times, is located in the area of Lettomanoppello village (Fig. 1, 19). Impressive bitumen occurrences ("seepage") characterize the outcropping biocalcarenes of the *Lepidocyclina* calcarenite 2 unit along a major fracture zone (Fig. 20A, C). This quarry offers a noteworthy outcrop where it is possible to observe the architecture of the Oligo-Miocene reservoir.

The quarry exposes the *Lepidocyclina* Calcarenite 2 unit and the overlying hemipelagic marls unit. In particular, on the SW wall of quarry, it is well evident the interdigitation of distal ramp lithofacies of the *Lepidocyclina* calcarenite ramp represented by the horizontally bedded marly packstone to wackestone and the sigmoidal cross-bedded grainstone (Fig. 21A, B). The main constituents of the marly packstone to wackestone are planktonic foraminifera, small benthic foraminifera, bryozoans, bivalves, and subordinately echinoids and serpulids. Glauconitic grains infilling planktonic foraminifera chambers are common. The beds are homogenous because of the *Thalassinoides*' bioturbation traces. Thickness ranges between 10 to 30 cm. The beds are separated by 1.5 cm thick interval rich in clayey marls. The cross-bedded grainstone consists of a skeletal debris made of bryozoans and echinoids. Larger benthic foraminifera are still present. These cross-beds are inclined between 10 and 22°; the dip is generally toward WNW. The first order sets are 20–60 cm thick. The sets are characterized by bedding-parallel lamination (bedding-plane discordant). The cosets (second order) are up to 5 m thick and are bounded by flat surfaces. The horizontal bedding style and the absence of cross-bedding in the marly packstone and wackestone lithofacies are indicative of deposition in low hydrodynamic conditions, the increasing of bioturbation, coupled with abundance of planktonic components, are typical of deposition in the distal outer ramp. On the contrary, the cross-bedded grainstone was produced by the migration of large, compound dunes in the distal portion of the middle ramp. The Valle Romana Quarry outcrop allows to observe the interfingering between middle and outer ramp environments.



The vertical alternation of these two lithofacies represents the intervals characterized by the migration of the dune on the distal sediment of the outer ramp, alternating with intervals during which is predominant decreasing and interruption of sediment transport and decay of dune fields (Brandano et al., 2012).

This quarry also represents an excellent place to observe the structure of two oblique normal faults (Fig. 19A). This exceptional exposure made this quarry one of the most studied sites for fluid flow analysis in fractured systems (e.g., Agosta et al., 2009, 2010; Zambrano et al., 2019; Volatili et al., 2019; Romano et al., 2020). Most of the fault planes recognized in the outcrops are mainly northwest-southeast-trending normal faults (Vezzani and Ghisetti, 1998; Agosta et al., 2009; Romano et al., 2020) where some minor left lateral movements

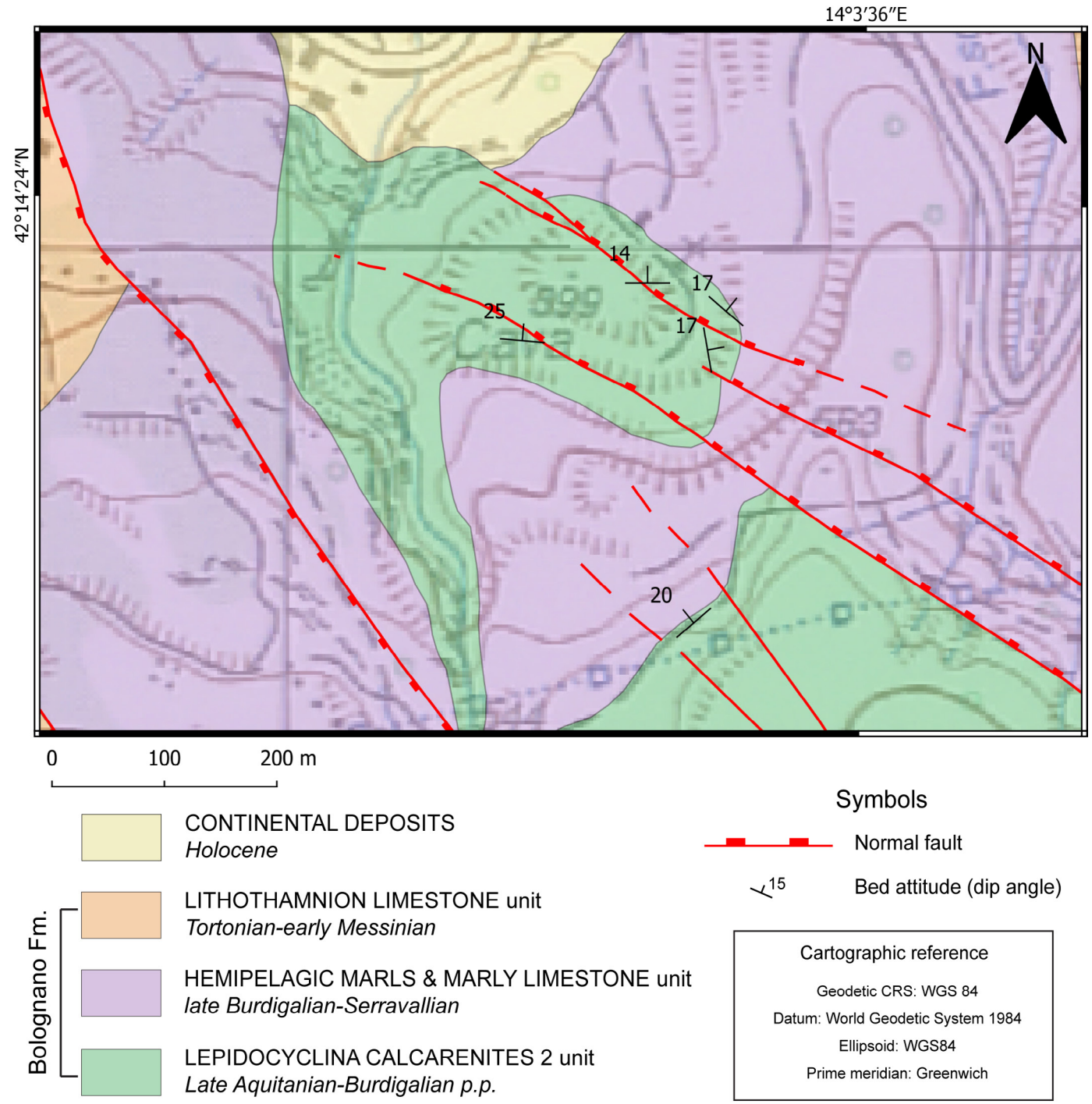


Fig. 19: Geological map of Valle Romana Quarry area.



are locally recognized (Agosta et al., 2010; Brandano et al., 2013). In particular, the SW fault dips 75° N and it is characterized by two main slip planes $\sim N290^\circ$ and $\sim N300^\circ$ (Agosta et al., 2010) with 40 m of throw. The NE fault is oriented $\sim N270^\circ$ to $\sim N315^\circ$, dipping 60° to 80° either N or S with about 10 m of throw. This fault pattern is considered the result of post-early Pliocene tectonic activity (Monaco et al., 1998; Ghisetti and Vezzani, 2002). Agosta et al. (2009) deeply studied the fault rocks outcropping in this quarry. They documented predominant pressure solution-based deformation and shearing

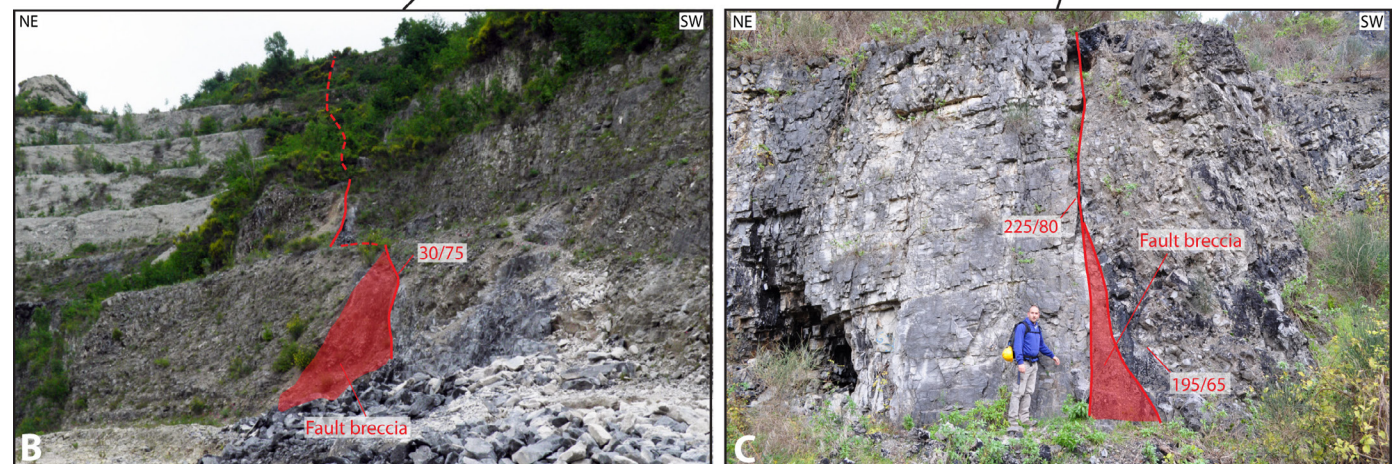
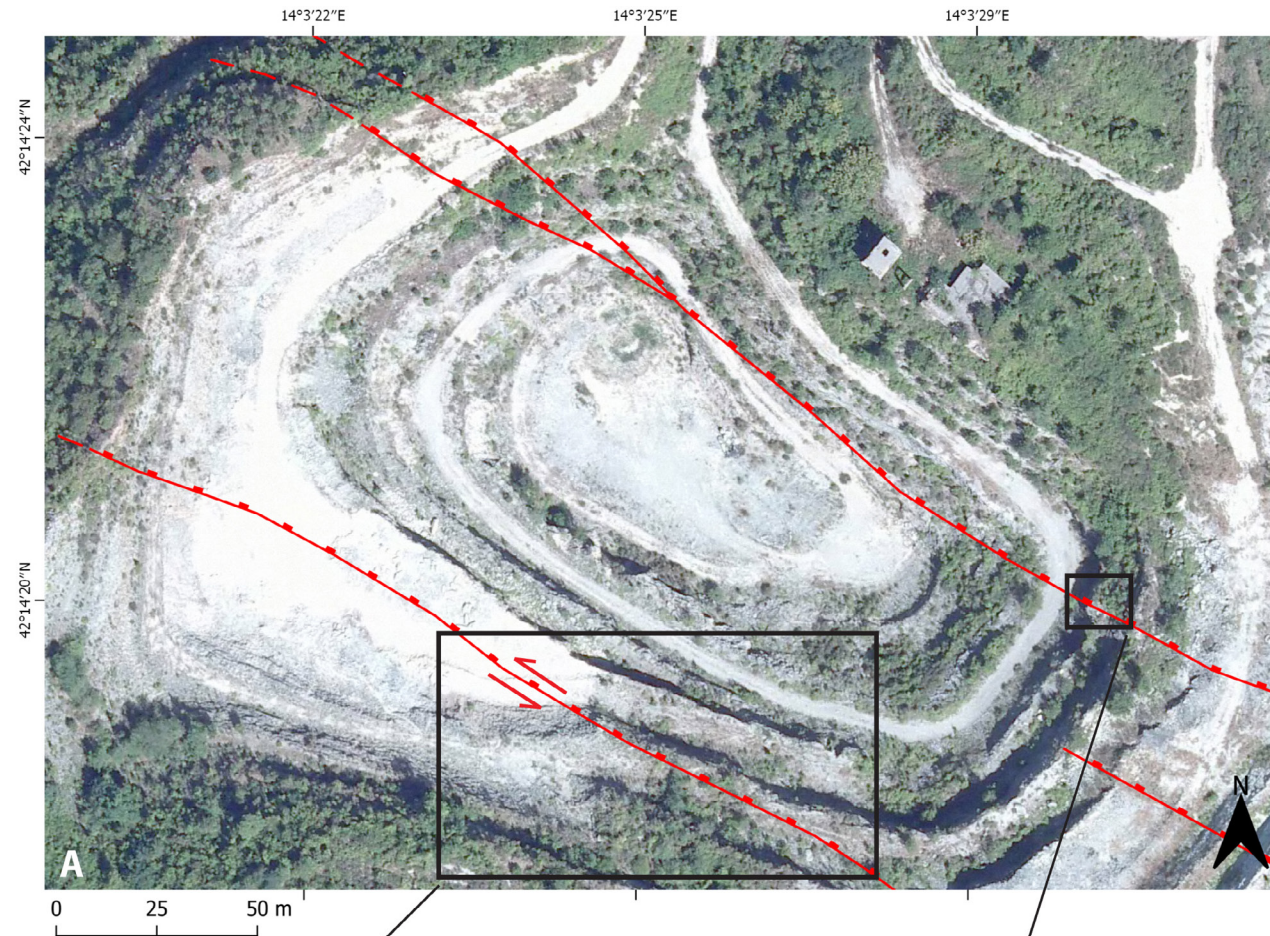


Fig. 20: A) Ortophoto of the Valle Romana Quarry. The line drawing shows the two large faults of the Roman Valley Quarry. B) SW fault in the Valle Romana Quarry. SW fault is oriented ca. $N290^\circ E$, dipping about 70° and with a vertical throw of about 40 m. C) NE fault in the Valle Romana Quarry. NE fault is nearly sub-vertical, oriented NW-SE striking fault zone, with ca. 10 m of displacement.

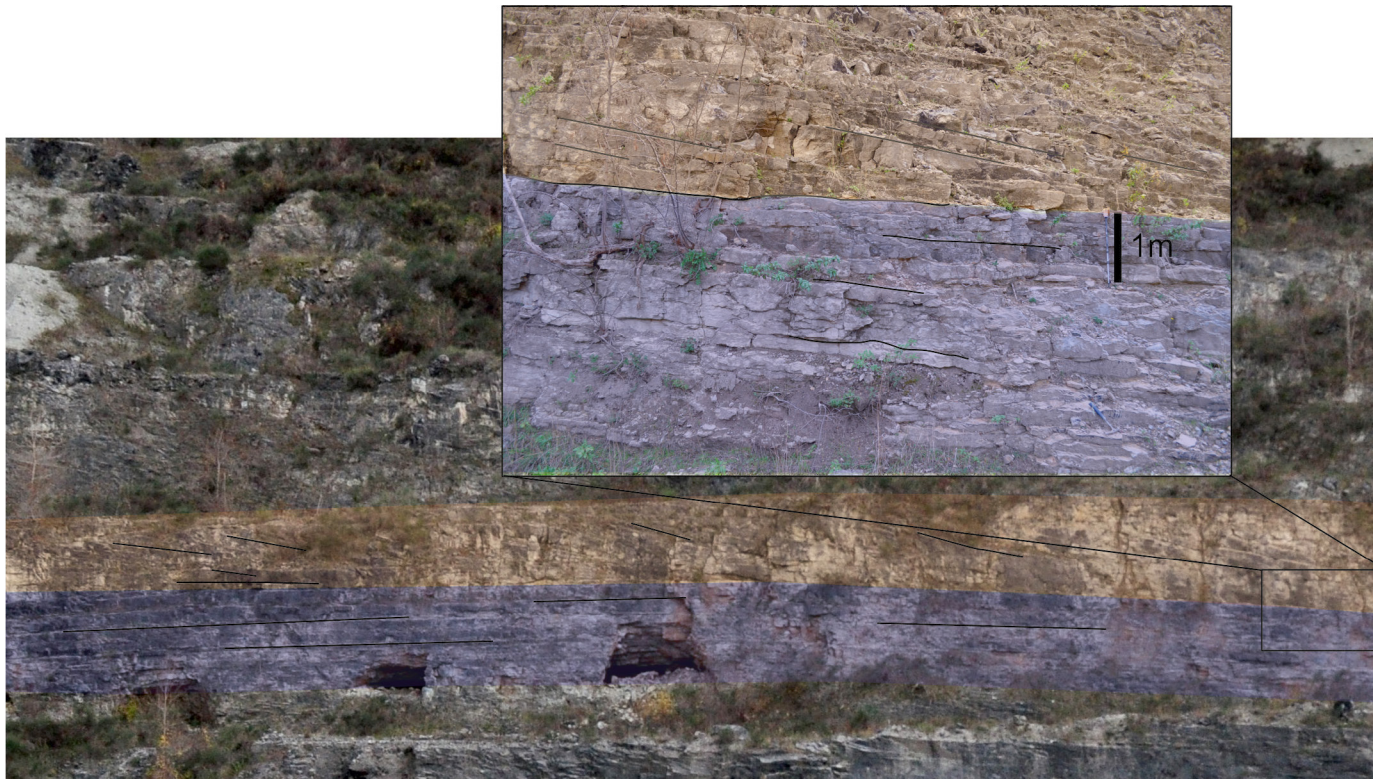


Fig. 21: The *Lepidocyclina* Calcarenite 2 is characterized by two main lithofacies in the Valle Romana Quarry: the horizontal bedded marly packstone and wackestone (blue) and the cross-bedded grainstone (orange), produced by the migration of large, compound dunes on the distal portion of the middle ramp represented by the marly deposits.

of pre-existing discontinuities during the processes of fault initiation, and intensive jointing, dilation of the pre-existing structural discontinuities and cataclasis during the subsequent fault growth. The resulting fault architecture is comprised of an inner core of cataclastic rocks and brecciated carbonates surrounded by fractured and faulted carbonate damage zones (Fig. 19 and 20). Field evidences clearly show that fault breccias and fault damage zones form conduits for fluid flow (Agosta et al., 2009, Brandano et al., 2013). It is worth noting that moving away from the fault zone, rock matrix still shows in some cases high hydrocarbon saturation being the matrix characterized by very high primary porosity (10-30%). This is in agreement to

what observed in the Acquafredda mines, where relatively undeformed and unfractured rocks quite distant from fault zones where anyway saturated. Starting from a very dense dataset of shallow wells data, Lipparini et al. (2018) observed that even if fault-related fractured zones show high hydrocarbon saturation, this happens only when these faults cut across hydrocarbon-bearing primary-porosity reservoirs. They thus suggested a local impact of faults in draining hydrocarbons that should mostly postdate the main migration of hydrocarbons within the reservoirs, being the last deformation phase post-early Pliocene and possibly late Pliocene to early Pleistocene (Vezzani and Ghisetti, 1998; Ghisetti and Vezzani, 2002). Trippetta et

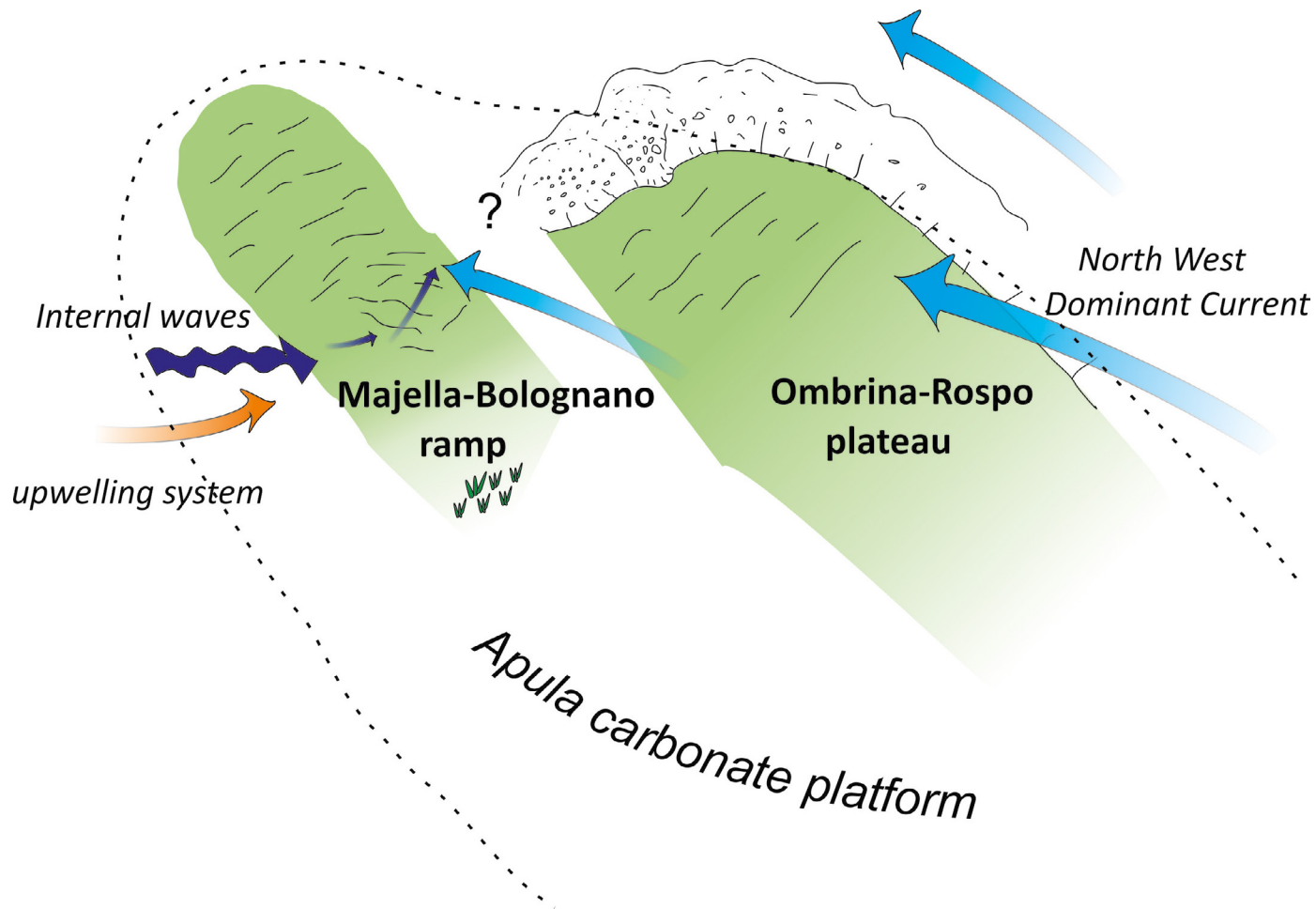


Fig. 22: Schematic paleogeography of northern Apulia carbonate platform and field dune development.

al. (2020) further suggested that this secondary oil migration was thus possibly driven from the high primary porosity and permeability of the Bolognano Fm. and due to its lateral continuity toward NW in agreement with Scrocca et al. (2013) that suggested the presence of the active source rocks in the northern areas where Triassic Evaporites are buried at larger depth.

Concluding remarks on dune field development

The 300-km wide proto-Adriatic sea was one of the largest seaways in the Mediterranean during the Burdigalian (Fig. 6) (Rögl, 1999; Dercourt et al., 2000; Popov et al., 2004). The eastern and the western boundaries of the proto-Adriatic sea were the Apulian carbonate ramp and by

the Dinaride coast. The southern portion of the proto-Adriatic sea faced the wide eastern part of the Mediterranean.

The paleoceanographic reconstructions in the northern extension of the proto-Adriatic suggest the presence of a northward current and an amphidromic system (de la Vara and Meijer, 2016). The tidal wave rotated counterclockwise around the amphidromic point creating tidal currents traveling to the northwest.



Interaction of the Mediterranean current and the tidal wave encroaching on the shallow-water Apulian ramp increased the flow speed. The accelerated current impinged bioclasts on the bottom producing the northwest migrating dunes (Fig. 2). However, northwest migrating dunes interbedded with 3-D northeast-directed dunes and phosphatic conglomerates rich of shark and fish teeth characterize the proximal portion of the middle ramp. Current research suggests these 3-D dunes may have been produced by internal waves propagated from the open southwestern portion of the proto-Adriatic sea and breaking on the northwestern sector of the Apulia ramp. Internal waves propagate along pycnoclines and are ubiquitous in the world oceans and lakes (Pomar et al., 2012, Pomar, 2020). Breaking internal waves or sloping surfaces causes a swash up-flow and a backwash return flow. The turbulence associated to the swash flow may produce erosion, and the backwash flow may produce transport of sediments downslope as bedload (Pomar et al., 2017; Pomar, 2020). However, the direction and the speed of the wash-up- and back-wash flows results from the wave energetics but also from the depositional dip angle of the ramp (Pomar et al., 2012, Pomar, 2020).

The internal waves are probably related to the upwelling system characterizing the Mediterranean and the Majella during the Burdigalian (Mutti and Bernoulli, 2003).

The presence of phosphatic conglomerates rich of shark and fish teeth interbedded in the cross-bedded succession testifies the occurrence of incipient hardgrounds related to upwelling currents propagating from the southwest to the northeast

Acknowledgments

The Editor in Chief Andrea Zanchi, the Associated Editor Domenico Chiarella and two anonymous reviewers are sincerely thanked for comments and suggestions that improved this manuscript. The Majella National Park, in particular Dr. Elena Liberatoscioli, is sincerely thanked for the license to work within the Park area. Juan Ignacio Baceta and Guillem Mateu Vicens are thanked for the useful discussion in the field.

References

- Agosta F., Alessandroni M., Tondi E., Aydin A. (2009) - Oblique normal faulting along the northern edge of the Majella Anticline, central Italy: Inferences on hydrocarbon migration and accumulation. *Journal of Structural Geology* 31, 674–690. <https://doi.org/10.1016/j.jsg.2009.03.012>.
- Agosta F., Alessandroni M., Antonellini M., Tondi E., Giorgioni M. (2010) - From fractures to flow: A field-based quantitative analysis of an outcropping carbonate reservoir. *Tectonophysics* 490, 197–213. <https://doi.org/10.1016/j.tecto.2010.05.005>
- Ashley G. M. (1990) - Classification of large-scale subaqueous bedforms; a new look at an old problem. *Journal of Sedimentary Research*, 60, 160-172.
- Aydin A., Antonellini M., Tondi E., Agosta F. (2010) - Deformation along the leading edge of the Maiella thrust sheet in central Italy. *Journal of Structural Geology*, 32, 1291–1304. <https://doi.org/10.1016/j.jsg.2008.10.005>
- Antonellini M., Tondi E., Agosta F., Aydin A., Cello G. (2008) - Failure modes in deep-water carbonates and their impact for fault development: Majella Mountain, Central Apennines, Italy. *Marine and Petroleum Geology*, 25(10), 1074-1096.
- Benedetti A., Di Carlo M., Pignatti J. (2010) - Embryo size variation in larger foraminiferal lineages: stratigraphy versus paleoecology in *Nephrolepidina praemarginata* (R. Douvillé, 1908) from the Majella Mt. (Central Apennines). *Journal of Mediterranean Earth Sciences*, 2, 19–29.
- Böhme M., Winklhofer M., Ilg, A. (2011) - Miocene precipitation in Europe: Temporal trends and spatial gradients. *Palaeogeography, Palaeoclimatology, Palaeoecology*, 304(3-4), 212-218.
- Bosellini A. (2002) - Dinosaurs “re-write” the geodynamics of the eastern Mediterranean and the paleogeography of the Apulia Platform. *Earth-Science Reviews*, 59(1-4), 211-234.
- Brandano M., Brillì M., Corda L., Lustrino M. (2010) - Miocene C-isotope signature from the central Apennine successions (Italy): Monterey vs. regional controlling factors. *Terra Nova*, 22(2), 125-130.
- Brandano M., Lipparini L., Campagnoni V., Tomassetti L. (2012) - Dowslope-migrating large dunes in the Chattian carbonate ramp of the Majella Mountains (Central Apennines, Italy). *Sedimentary Geology*, 255–256, 29–41.
- Brandano M., Scrocca D., Lipparini L., Petracchini L., Tomassetti L., Campagnoni V., Meloni D., Mascaro G. (2013) - Physical stratigraphy and tectonic settings of Bolognano Formation (Majella): A potential carbonate reservoir. *Journal of Mediterranean Earth Sciences*, 5, 151–176.
- Brandano M., Cornacchia I., Raffi I. and Tomassetti L. (2016a) - The Oligocene–Miocene stratigraphic evolution of the Majella carbonate platform (Central Apennines, Italy). *Sedimentary Geology*, 333, 1-14.
- Brandano M., Tomassetti L., Sardella R. Tinelli C. (2016c) - Progressive deterioration of trophic conditions in a carbonate ramp environment: the Lithothamnion Limestone, Majella Mountain (Tortonian–early Messinian, central Apennines, Italy). *Palaios*, 31(4), 125-140.
- Brandano M., Westphal H., Mateu-Vicens G., Preto N., Obrador A. (2016b) - Ancient upwelling record in a phosphate hardground (Tortonian of Menorca, Balearic Islands, Spain). *Marine and Petroleum Geology*, 78, 593-605.

- Brandano M., Cornacchia I., Raffi I., Tomassetti L., Agostini S. (2017) - The Monterey Event within the Central Mediterranean area: The shallow-water record. *Sedimentology*, 64, 286-310.
- Brandano M., Tomassetti L., Cornacchia I. (2019) - The lower Rupelian cluster reefs of Majella platform, the shallow water record of Eocene to Oligocene transition. *Sedimentary Geology*, 380, 21-30.
- Brandano M., Ronca S., Di Bella L. (2020) - Erosion of Tortonian phosphatic intervals in upwelling zones: The role of internal waves. *Palaeogeography, Palaeoclimatology, Palaeoecology*, 537, 109405.
- Burnett W.C., Roe K.K., Piper D.Z. (1983) - Upwelling and phosphorite formation in the ocean. In: Thiede, J., Suess, E. (Eds.), *Coastal Upwelling its Sediment Record*. Springer, Berlin, Heidelberg, pp. 377-397.
- Cahuzac B., Poignant A. (1997) - Essai de biozonation de l'Oligo-Miocène dans les bassins européens à l'aide des grands foraminifères néritiques. *Bulletin de la Societe Geologique de France*, 168, 155-169.
- Carnevale G., Patacca E. and Scandone P. (2011) Field guide to the post-conference excursions (Scontrone, Palena and Montagna della Majella). R.C.M.N.S. Interim Colloquium, 4-5 March 2011, Scontrone (L'Aquila), Italy, pp. 1-99.
- Cazzini F., Zotto O.D., Fantoni R., Ghielmi M., Ronchi P., Scotti P. (2015) - Oil and gas in the adriatic foreland, Italy. *J. Pet. Geol.*, 38, 255-279. <https://doi.org/10.1111/jpg.12610>
- Cornacchia I., Andersson P., Agostini S., Brandano M., Di Bella L. (2017) - Strontium stratigraphy of the upper Miocene Lithothamnion Limestone in the Majella Mountain, central Italy, and its palaeoenvironmental implications. *Lethaia*, 50(4), 561-575.
- Cornacchia I., Agostini S., Brandano M. (2018) - Miocene oceanographic evolution based on the Sr and Nd isotope record of the Central Mediterranean. *Paleoceanography and Paleoclimatology*, 33(1), 31-47.
- Cosentino D., Cipollari P., Marsili P., Scrocca D. (2010) Geology of the central Apennines: a regional review. In: *The Geology of Italy* (Eds M. Beltrando, A. Peccerillo, M. Mattei, S. Conticelli and C. Doglioni). Journal of the Virtual Explorer, Electronic Edition, 36, paper 11. ISSN 1441-8142.
- Crescenti U., Crostella A., Donzelli G., Raffi G. (1969) Stratigrafia della serie calcarea dal Lias al Miocene nella regione marchigiana abruzzese: Parte II. Litostratigrafia, biostratigrafia, paleogeografia. *Memorie della Società Geologica Italiana*, 9, 343-420.
- de la Vara A. and Meijer P. (2016) - Response of Mediterranean circulation to Miocene shoaling and closure of the Indian Gateway: A model study. *Palaeogeography, Palaeoclimatology, Palaeoecology*, 442, 96-109.
- de la Vara A., Meijer P. T., Wortel M.J.R. (2013) - Model study of the circulation of the Miocene Mediterranean Sea and Paratethys: closure of the Indian Gateway. *Climate of the Past Discussions*, 9(4).
- Dall'Antonia B. (2003) - Deep-sea ostracods as indicators of palaeoceanographic changes: a case from the middle-late Miocene of southern Italy (Central Mediterranean). *Terra Nova*, 15, 52-60.
- Dercourt J., Gaetani M., Vrielynck B., Barrier E., Biju-Duval B., Brunet M.F., Cadet J.P., Crasquin S., Sandulescu M. (2000) - *Peri-Tethys Atlas: Palaeogeographical Maps*. Comm. for the Geol. Map of the World, Paris.
- Di Cuia R., Shakerley A., Masini M., Casabianca D. (2009) - Integrating outcrop data at different scales to describe fractured carbonate reservoirs: example of the Maiella carbonates, Italy. *First Break* 27, 45-55. <https://doi.org/10.3997/1365-2397.2009006>
- Doglioni, C. (1994) - Foredeeps versus subduction zones. *Geology*, 22, 271-274.

- Eberli G.P., Bernoulli D., Sanders D., Vecsei A. (1993) - From aggradation to progradation: the Maiella platform, Abruzzi Italy. In: Cretaceous Carbonate Platforms (Simo T., Scott R.W., Masse J.P. Eds.), AAPG Memoir, 56, 213–237.
- Eberli G.P., Bernoulli D., Vecsei A., Sekti R., Grasmueck, M., Lüdmann T., Anselmetti F.S., Mutti M. and Della Porta G. (2019) A Cretaceous carbonate delta drift in the Montagnadella Maiella, Italy. *Sedimentology*, 66, 1266–1301.
- Föllmi K. B. (1996). The phosphorus cycle, phosphogenesis and marine phosphate-rich deposits. *Earth -Science Reviews*, 40(1-2), 55-124.
- Föllmi K.B., Gertsch B., Renevey J. P., De Kaenel E., Stille, P. (2008) - Stratigraphy and sedimentology of phosphate-rich sediments in Malta and south-eastern Sicily (latest Oligocene to early Late Miocene). *Sedimentology*, 55(4), 1029-1051.
- Föllmi K.B., Hofmann H., Chiaradia M., de Kaenel E., Frijia G., Parente, M. (2015) - Miocene phosphate-rich sediments in Salento (southern Italy). *Sedimentary Geology*, 327, 55-71.
- Gebhardt H. (1999) - Middle to Upper Miocene benthonic foraminiferal palaeoecology of the Tap Marls (Alicante Province, SE Spain) and its palaeoceanographic implications. *Palaeogeography, Palaeoclimatology, Palaeoecology*, 145(1-3), 141-156.
- Gerali F. (2013) - Imprenditoria e scienza nell'industria petrolifera abruzzese del XIX secolo. *Energia* 2, 50–55.
- Gerali F. and Lipparini L. (2018) - Maiella, an oil massif in the Central Apennines ridge of Italy: Exploration, production and innovation in the oil fields of Abruzzo across the nineteenth and twentieth centuries. *Geological Society Special Publication*, 465, 275–303. <https://doi.org/10.1144/SP465.20>
- Ghisetti F. and Vezzani, L. (2002) - Normal faulting, extension and uplift in the outer thrust belt of the central Apennines (Italy): Role of the Caramanico fault. *Basin Research*, 14, 225–236. <https://doi.org/10.1046/j.1365-2117.2002.00171.x>
- Graham B., Antonellini M., Aydin A. (2003) - Formation and growth of normal faults in carbonates within a compressive environment. *Geology*, 31(1), 11-14.
- Houben A.J., van Mourik C.A., Montanari A., Coccioni R., Brinkhuis H. (2012) - The Eocene–Oligocene transition: changes in sea level, temperature or both? *Palaeogeography, Palaeoclimatology, Palaeoecology*, 335, 75–83.
- Iadanza A., Sampalmieri G., Cipollari P. (2015) - Deep-seated hydrocarbons in the seep “Brecciated Limestones” of the Maiella area (Adriatic foreland basin): Evaporitic sealing and oil re-mobilization effects linked to the drawdown of the Messinian Salinity Crisis. *Marine and Petroleum Geology*, 66, 177–191. <https://doi.org/10.1016/j.marpetgeo.2015.03.006>
- Jervis G. (1873) - *I tesori sotterranei dell'Italia*. Loescher, Torino.
- Lavenu A.P.C.C., Lamarche J., Salardon R., Gallois A., Marié L., Gauthier B.D.M.M. (2014) - Relating background fractures to diagenesis and rock physical properties in a platform-slope transect. Example of the Maiella Mountain (central Italy). *Marine and Petroleum Geology*, 51, 2–19. <https://doi.org/10.1016/j.marpetgeo.2013.11.012>
- Karami M.P., Meijer P.T., Dijkstra H.A., Wortel M.J.R. (2009) - An oceanic box model of the Miocene Mediterranean Sea with emphasis on the effects of closure of the eastern gateway. *Paleoceanography*, 24(4).
- Kocsis L., Vennemann T. W., Fontignie D., Baumgartner C., Montanari A., Jelen B. (2008) - Oceanographic and climatic evolution of the Miocene Mediterranean deduced from Nd, Sr, C, and O isotope compositions of marine fossils and sediments. *Paleoceanography*, 23(4).

- Lipparini L., Trippetta F., Ruggieri R., Brandano M., Romi A. (2018) - Oil distribution in outcropping carbonate-ramp reservoirs (Maiella Mountain, Central Italy): Three-dimensional models constrained by dense historical well data and laboratory measurements. *AAPG Bulletin*, 102(7), 1273-1298.
- Magini M. (1977) - *L'Italia e il petrolio tra storia e cronologia*. Mondadori, Vicenza.
- Marchegiani L., Van Dijk J.P., Gillespie P.A., Tondi E., Cello G. (2006) - Scaling properties of the dimensional and spatial characteristics of fault and fracture systems in the Majella Mountain, central Italy. In: Cello G., Malamud B. (Eds.), *Fractal Analysis for Natural Hazards*. Geological Society of London, Special Publication, 261, 113-131. <https://doi.org/10.1144/GSL.SP.2006.261.01.09>
- Monaco C., Tortorici L., Paltrinieri W. (1998) - Structural evolution of the Lucanian Apennines, southern Italy. *Journal of Structural Geology*, 20, 617-638. [https://doi.org/10.1016/S0191-8141\(97\)00105-3](https://doi.org/10.1016/S0191-8141(97)00105-3)
- Moussavian E. and Vecsei A. (1995) - Paleocene reef sediments from the Maiella carbonate platform, Italy. *Facies*, 32, 213-221.
- Mutti M. and Bernoulli D. (2003) - Early marine lithification and hardground development on a Miocene ramp (Maiella, Italy): key surfaces to track changes in trophic resources in nontropical carbonate settings. *Journal of Sedimentary Research*, 73, 296-308.
- Mutti M. and Hallock P. (2003) - Carbonate systems along nutrient and temperature gradients: some sedimentological and geochemical constraints. *International Journal of Earth Sciences*, 92(4), 465-475.
- Mutti M., Bernoulli D., Stille P. (1997) - Temperate carbonate platform drowning linked to Miocene oceanographic events: Maiella platform margin, Italy. *Terra Nova*, 9, 122-125.
- Novelli L. and Sella M. (2009) - *Il petrolio: una storia antica*. Silvana Editoriale, Cinisello Balsamo.
- Okay A.I., Zattin M., Cavazza W. (2010) - Apatite fission-track data for the Miocene Arabia-Eurasia collision. *Geology*, 38(1), 35-38.
- Patacca E., Scandone P., Di Luzio E., Cavinato G.P., Parotto M. (2008) - Structural architecture of the central Apennines: interpretation of the CROP 11 seismic profile from the Adriatic coast to the orographic divide. *Tectonics*, 27, TC3006 (36 pp.).
- Pedley H.M. and Bennett S.M. (1985) - Phosphorites, hardgrounds and syndepositional solution subsidence: a palaeoenvironmental model from the Miocene of the Maltese Islands. *Sedimentary Geology*, 45(1-2), 1-34.
- Pomar L. (2020) Chapter 12 - Carbonate systems. In: *Regional Geology and Tectonics (Second Edition)* (Eds N. Scarselli, J. Adam, D. Chiarella, D.G. Roberts and A.W. Bally), pp. 235-311. Elsevier.
- Pomar L., Baceta J.I., Hallock P., Mateu-Vicens G., Basso D. (2017) - Reef building and carbonate production modes in the west-central Tethys during the Cenozoic. *Marine and Petroleum Geology* 83, 261-304.
- Pomar L., Brandano M., Westphal H. (2004) - Environmental factors influencing skeletal grain sediment associations: a critical review of Miocene examples from the western Mediterranean. *Sedimentology*, 51, 627-651.
- Pomar L., Morsilli, M., Hallock, P. and Bádenas, B. (2012) Internal waves, an under-explored source of turbulence events in the sedimentary record. *Earth-Science Reviews*, 111, 56-81.
- Popov S.V., Rögl F., Rozanov A.Y., Steininger F.F., Shcherba I.G., Kovac M. (2004) - Lithological-paleogeographic maps of Paratethys. Late Eocene to Pliocene. In S. V. Popov, et al. (Eds.), *Courier Forschungsinstitut Senckenberg* (Vol. 250, 46 pp.), maps 1-10 (annex).

- Rögl F. (1999) - Mediterranean and Paratethys. Facts and hypotheses of an Oligocene to Miocene paleogeography (short overview). *Geologica Carpathica*, 50(4), 339-349.
- Romano V., Bigi S., Carnevale F., De'Haven Hyman J., Karra S., Valocchi A.J., Tartarello M.C., Battaglia M. (2020) - Hydraulic characterization of a fault zone from fracture distribution. *Journal of Structural Geology*, 135, 104036. <https://doi.org/10.1016/j.jsg.2020.104036>
- Rusciadelli G., Sciarra N., Mangifesta M. (2003) - 2D modelling of large-scale platform margin collapses along an ancient carbonate platform edge (Maiella Mt., Central Apennines, Italy): geological model and conceptual framework. *Palaeogeography, Palaeoclimatology, Palaeoecology*, 200(1-4), 245-262.
- Rustichelli A., Tondi E., Agosta F., Cilona A., Giorgioni M. (2012) - Development and distribution of bed-parallel compaction bands and pressure solution seams in carbonates (Bolognano Formation, Majella Mountain, Italy). *Journal of Structural Geology*, 37, 181-199.
- Scisciani V., Tavarnelli E., Calamita F. (2002) - The interaction of extensional and contractional deformations in the outer zones of the Central Apennines, Italy. *Journal of Structural Geology*, 24, 1647-1658.
- Scrocca D., Inversi B., Lipparini L. (2011) - A Review of Petroleum Plays in the Meso-Cenozoic Carbonates in Central Adriatic Sea (Italy). AAPG Search and Discovery Article, 90135, AAPG International Conference.
- Scrocca D., Brandano M., Petracchini L., Lipparini L. (2013) - Analysis of an exhumed oil accumulation: the Oligo-Miocene carbonate ramp deposits of the Majella Mountain (Central Italy). AAPG-ER Newsletter, 8, 2-4.
- Tondi E., Antonellini M., Aydin A., Marchegiani L., Cello P. (2006) - The roles of deformation bands and pressure solution seams in fault development in carbonate grainstones of the Majella Mountain, Italy. *Journal of Structural Geology*, 28, 376-391.
- Trippetta F., Ruggieri R., Brandano M., Giorgetti C. (2020) - Petrophysical properties of heavy oil-bearing carbonate rocks and their implications on petroleum system evolution: Insights from the Majella Massif. *Marine and Petroleum Geology*, 111, 350-362.
- Vecsei A. and Moussavian E. (1997) - Paleocene reefs on the Maiella platform margin, Italy: an example of the effects of the Cretaceous/Tertiary boundary events on reefs and carbonate platforms. *Facies*, 36, 123.
- Vecsei A. and Sanders D.G. (1999) - Facies analysis and sequence stratigraphy of a Miocene warm-temperate carbonate ramp, Montagna della Maiella, Italy. *Sedimentary Geology*, 123, 103-127.
- Vecsei A., Sanders D.G., Bernoulli D., Eberli G.P., Pignatti J.S. (1998) - Cretaceous to Miocene sequence stratigraphy and evolution of the Maiella carbonate platform margin, Italy. In: *Mesozoic and Cenozoic Sequence Stratigraphy of European Basins* (Hardenbol, J., Thierry, J., Farley, M.B., Jacquin, T., De Graciansky, P.C., Vail, P.R. Eds.), SEPM Special Publication, 60, 53-74.
- Vescogni A., Vertino A., Bosellini F.R., Harzhauser M., Mandic O. (2018) - New paleoenvironmental insights on the Miocene condensed phosphatic layer of Salento (southern Italy) unlocked by the coral-mollusc fossil archive. *Facies* 64, 7. <https://doi.org/10.1007/s10347-018-0520-9>
- Vezzani L. and Ghisetti F. (1998) - Carta geologica dell'Abruzzo, 1: 100000. SELCA, Florence, Italy.
- ViDEPI Project (2007) - Visibility of Petroleum Exploration Data in Italy [WWW Document]. Ital. Minist. Econ. Dev. URL <https://unmig.mise.gov.it/videpi/videpi.asp>

- Vitale S., Amore O.F., Ciarcia S., Fedele, L. Grifa, C. Prinzi, E.P., Tavani S., Tramparulo F.D.A. (2018) - Structural, stratigraphic, and petrological clues for a Cretaceous–Paleogene abortive rift in the southern Adria domain (southern Apennines, Italy). *Geological Journal*, 53(2), 660-681.
- Volatili T., Zambrano M., Cilona A., Huisman B.A.H., Rustichelli A., Giorgioni M., Vittori S., Tondi E. (2019) - From fracture analysis to flow simulations in fractured carbonates: The case study of the Roman Valley Quarry (Majella Mountain, Italy). *Marine and Petroleum Geology*, 100, 95-110.
- Zachos J., Pagani M., Sloan L., Thomas E., Billups K. (2001) - Trends, rhythms, and aberrations in global climate 65 Ma to present. *Science*, 292(5517), 686-693.
- Zambrano M., Pitts A.D., Salama A., Volatili T., Giorgioni M., Tondi E. (2019) - Analysis of fracture roughness control on permeability using SFM and fluid flow simulations: Implications for carbonate reservoir characterization. *Geofluids* 2019. <https://doi.org/10.1155/2019/4132386>

Manuscript received 06 September 2020; accepted 7 November 2020; published online 10 December 2020; editorial responsibility and handling by D. Chiarella.